SUPERSONIC WING-BODY INTERFERENCE

Thesis by

Jack Norman Nielsen

In Partial Fulfillment of the Requirements

For the Degree of

Doctor of Philosophy

California Institute of Technology

Pasadena, California

1951

ACKNOWLEDGEMENTS

The writer would like to acknowledge his gratitude to Professor P. A. Lagerstrom under whose supervision this thesis was accomplished. Professor Lagerstrom's interest was heartening, and his advice and criticism were invaluable. The lectures of Professor M. Ward inspired the interest in mathematical analysis that made this thesis possible. Professors C. De Prima, A. Erdelyi, and F. Tricomi were very kind in extending helpful mathematical advice. The author would also like to acknowledge the contribution of the National Advisory Committee for Aeronautics in whose Ames Laboratory the characteristic functions were computed under the able supervision of Mrs. J. Stalder.

ABSTRACT

A method of solving wing-body problems for circular bodies employing wings with supersonic edges has been developed. The method is based on decomposing the wing-body combination into a wing alone plus a number of Fourier component wing-body combinations corresponding to the Fourier series for the normal velocity induced at the body surface by the wing alone. The problem is then solved for each component by a method based on Laplace transform theory, and the method is then shown to be equivalent to a distributed-solution method analogous to that used by Karman and Moore to solve problems of bodies of revolution at supersonic speeds. Two sets of universal functions are presented. The first set is used to obtain the strength distribution of the fundamental solutions distributed along the body axis, from which the entire interference pressure field can be obtained. The second set permits a direct determination of the pressures acting on the body.

As an example in the use of the theory, calculations are carried out for the technologically important case of a flat rectangular wing mounted at zero incidence on a body at zero angle of attack. The calculations are carried out for four Fourier components. It was found that all four components were necessary to get good accuracy in determining the pressures at some points in the field,

while only one component was required to get a fair determination of the span loading of the combination. From the example much insight into the mechanism of wing-body interference was obtained. The use of the universal functions to obtain pressures due to protuberances on nearly cylindrical bodies is discussed.

TABLE OF CONTENTS

TABLE OF CONTENTS (Cont'd)

SYMBOLS

a	body radius
AR	wing aspect ratio
$a_{2n}(z)$, $b_{2n}(z)$, $c_{2n}(z)$	functions of z used in Appendix
$C(z)$, $C^*(z)$	Fourier cosine transforms
C_0, C_1, ---C_4	polynomials in n
C_2^*, C_4^* , C_6^*	polynomials in n
C_P	pressure coefficient
$C_{P_{2n}}$	pressure coefficient of n'th Fourier component
E	error in determination of $M_{2n}(z)$
E^*	error in determination of $W_{2n}(z)$
E_ν	Weber or Lommel-Weber function of order ν
$f_{2n}(z)$	amplitude of body normal velocity due to n'th Fourier component
$F_{2n}(s)$	Laplace transform of $f_{2n}(s)$
$g_{2n}^{(2n-1)}(z)$	strength function for axial distribution of n'th Fourier component
$G_{2n}^{(2n-1)}(s)$	Laplace transform of $g_{2n}^{(2n-1)}(z)$
$h_{2n}(z,r)\cos 2n\theta$	fundamental solution
$H_{2n}^{(1)}(z)$	Hankel function of first kind and 2n'th order
$I_{2n}(\tau)$, $I_{2n}^*(\tau)$	amplitudes of integrands of Fourier integrals
$I_m(z)$	modified Bessel function of first kind of order m
$J_\nu(z)$	Anger function, equivalent to usual Bessel function for integral values of ν .
$J_{2n}(z)$	Bessel function of first kind of order 2n
K^*, K	kernels of integral equations

SYMBOLS (Cont'd)

$K_m(z)$	modified Bessel function of second kind of order m
ΔL_{2n}	lift on wing due to n'th Fourier component
M	free-stream Mach number
m	cotangent of leading edge sweepback angle, summation index
$M_{2n}(z)$	characteristic function
n	number of Fourier component
p	local static pressure
p_o	free-stream static pressure
Δp_{2n}	loading per unit area due to n'th Fourier component
q	free-stream dynamic pressure
q*	normal velocity at body surface due to wing potential
r, θ, z	cylindrical coordinates
s	complex variable of Laplace transform plane
S(z), S * (z)	Fourier sine transforms
t	complex variable,
V_o	free-stream velocity
$W_{2n}(z)$	characteristic function
x, y, z	Cartesian coordinates
$Y_{2n}(z)$	Bessel function of second kind of order 2n
α_B	body angle of attack
α_u	upwash angle of flow due to body
α_W	wing angle of attack
ϕ	velocity potential, interference perturbation velocity potential

SYMBOLS (Cont'd)

Φ	transformed interference potential
ϕ_{2n}	interference potential of n'th Fourier component
Φ_{2n}	Laplace transform of ϕ_{2n}
ϕ_W	wing alone velocity potential
ξ	variable of integration
ρ	mass density in free stream
τ	upper limit of integration
ψ	$\cos^{-1}\sqrt{1-z^2}$
$\Gamma(n+1)$	gamma function, n!

I. INTRODUCTION

1.1 Preliminary Remarks

An explanation of the term "interference" as used herein will first be given. Consider a geometric body immersed in a fluid field of infinite extent with a uniform velocity at distances infinitely far from the body. As a result of the curvature of the paths of the fluid particles in the field pressure gradients will be set up in the fluid. Consider now a different body under similar circumstances. A second pressure field will be associated with this body. If both bodies are considered simultaneously to be in the fluid, the pressure field set up will differ from the sums of the body-alone pressure fields. The difference arises from the fact that the velocities set up by one body acting alone will not in general be tangential to the other body. The difference between the joint pressure field and the sum of the body-alone pressure fields is known as the interference pressure field. The term "interference" can be applied to aerodynamic quantities such as lift, moment, drag, pressure, etc.

In cases where two distinct bodies are under consideration, the definition of what constitutes the interference is not hard. However in cases where a complicated body is formed by the coalescence of two or more simpler bodies, the specification of the interference is quite arbitrary because the decomposition of the complicated body into simpler bodies is not unique. For instance, a wing-

body combination is formed from a wing alone and a body alone. But the wing can be continued through the body in many ways without affecting the external shape of the wing-body combination. However it can be said that no matter how the wing alone is defined, the sum of the wing-alone, body-alone, and interference pressure fields will be unique in so far as the external flow past the wing-body combination is unique. It is reasonable, therefore, to define the wing alone in the manner best suited to the problem at hand.

Aircraft designers have been cognizant practically from the advent of the airplane of the important effects that interference among the various parts of the airplane can have on its performance and efficiency. However for low-speed flight where the governing differential equation is Laplace's equation, no solutions for a three-dimensional wing-body combination have yet been found. This is a direct consequence of the mathematical complexity of the problem. Practically the effects of interference were evaluated by wind-tunnel tests of models of the design under consideration. In many instances the aspect ratio of the wings was sufficiently large so that no important effects of interference were encountered, and frequently where adverse effects were met, they could be alleviated by suitable fairing of the wing-body juncture. However for supersonic aircraft the trend is toward wings of low

aspect ratio for which interference effects can be very important. Also the properties of the governing differential equation are such that some hope of obtaining mathematical solutions exists. For these reasons the problems of wing-body interference for supersonic flight have received much attention from aeronautical scientists and engineers in recent years.

In attempting to solve the problems of fluid flow past bodies at rest it is common to utilize the partial differential equations governing the velocity potential which exists for an inviscid fluid, either compressible or incompressible. In the incompressible case the equation is Laplace's equation. For wings the problem is further linearized by specifying the boundary conditions for the potential not at the wing surface but rather in a plane called the plane of the wing. For compressible fluid the differential equation is non-linear, and it is usually linearized on the assumption of small perturbation velocities to give the wave equation. In this paper the wave equation will be used, the boundary conditions for the wing will be applied in the plane of the wing, and the body boundary conditions will be applied at the surface of the unit cylinder.

1.2 Present Status of Problem

One of the boundary-value problems of interference that has been attempted is that of supersonic flow past an inclined pointed body of revolution with a flat rectangular wing (Reference 1). The

wing was first assumed to be imbedded in the flow field of the body alone and the pressures acting on it were determined. Then to get the interference pressures on the body, the body was assumed to be imbedded in the flow field of the wing alone. As a result of these assumptions, the results of Reference (1) represent a first approximation to the interference pressure field. In Reference (2) certain errors of Reference (1) are corrected.

In order to gain insight into the phenomena of interference, several authors have sought to make interference problems more tractable by the expedient of simplifying either the geometry or the differential equation. Following the first line of attack, Browne, Friedman and Hodes in Reference (3) attempt the solution of the pressure field acting on a wing-body combination composed of a flat triangular wing and a conical body having a common apex. The use of all-conical boundaries reduces the problem to one of conical flow for which powerful methods of solution are available (Reference 4). This combination is thus of considerable theoretical interest.

The second expedient of simplifying the differential equation has led to some simple and useful results. The velocity potential for linearized supersonic flow is governed by the wave equation

$$(M^2-1)\,\phi_{zz} - \phi_{xx} - \phi_{yy} = 0 \qquad (1)$$

where M is the free-stream Mach number. Under certain circumstances the first term of Equation (1) can be neglected compared to the second and third terms so as to give Laplace's equation. This simplification leads to so-called slender-body theory. The assumption is valid in certain instances for Mach numbers near unity and for bodies slender in the flight direction. Spreiter in Reference (5) has discussed slender-body theory and has applied it to triangular wings on pointed slender bodies of revolution. In Reference (6) Spreiter has applied the theory to combinations with cruciform wings.

In his doctoral thesis Morikawa (Reference 7) has presented an approximate solution for the case of a rectangular wing and a circular body both inclined at the same angle of attack. The method of solution is based on the use of Laplace transform theory together with approximate expressions for the Green's function. Morikawa concludes "The analytical work has just begun on non-planar problems".

In Reference (8) Nielsen and Matteson present a numerical technique for obtaining the pressure field on the wing for a combination composed of a body at zero angle of attack and a wing for which the interaction between upper and lower surfaces has no effect on the interference.

In Reference (9) Lagerstrom and Van Dyke have discussed

many aspects of the wing-body interference problem. In addition to planar systems, they have considered non-planar systems utilizing polygonal bodies. An approximate method based on strip theory is given, and the more exact methods available for circular bodies are outlined.

1.3 Purpose of Present Study

It is the purpose of this report to continue the analytical work that has already been started in the realm of non-planar problems. From the outset it was realized that the inherent analytical difficulties of non-planar problems make the prospect of obtaining simple closed solutions remote. The question thus reduces to one of obtaining a solution in some other convenient form. A Fourier series solution giving good accuracy for a few terms was used. The method of solution depends primarily on a set of universal characteristic functions solving a wide class of interference problems (as well as such problems as pressures due to protuberances on near-circular fuselages). The properties of these functions are discussed and their numerical values are tabulated for purposes of computation. As an example of the application of the theory, the technologically important case of a flat rectangular wing mounted on a circular body at zero angle of attack is carried out. From this example some useful deductions concerning the mechanism of interference are obtained. Furthermore "exact" solutions are very useful

as yardsticks by which to measure the degree of validity of the semi-empirical methods of determining wing-body interference that are arising, and to evaluate the correctness of their underlying assumptions. Throughout the thesis, the analytical complexity of the problem should be borne in mind.

II. FORMAL SOLUTION OF PROBLEM

2.1 Basic Preliminary Considerations

Prior to the direct mathematical formulation of the boundary value problems considered herein, some physical discussion of the problems will be given. Throughout the governing differential equation is Equation (1); and furthermore, the free-stream Mach number is specialized to $\sqrt{2}$ without any loss of generality. No effect of wing tips will be considered.

A typical wing-body combination can be thought of as composed of a nose, winged section, and afterbody as shown in Figure (1). In general the body will be inclined at an angle of attack different from that of the wing, which may be cambered and twisted. Over the nose of the combination the problem is essentially one of a body of revolution, and it can be solved by the methods of References (10) or (11). The essential boundary conditions are that the flow be uniform in front of the nose, and that it be everywhere tangent to the body; that is, $\frac{\partial \phi}{\partial n}$ be zero at the body surface.

No interference is encountered until the flow reaches the winged portion of the wing-body combination since disturbances can be propagated only downstream within their Mach cones. The effect of interference will be felt on the body only behind the forward boundary of the region of influence of the wings on the body. This forward boundary can easily be seen to correspond to the

downstream helices originating at the leading-edges of the wing-body junctures and lying on the body surface, intersecting all parallel elements of the cylinder at the Mach angle. It is clear that the helices intersect at the top and bottom of the body a distance $\pi a \sqrt{M^2-1}/2$ downstream from the leading edge of the juncture. For greater distances downstream the wing influences the body around its entire circumference.

A further significant boundary for the winged part of the combination is that delineating the region of influence of one half-wing on the other. Consider a disturbance propagated from the leading edge of the left wing-body juncture up the helix to the top of the body. The disturbance can continue downward along the helix or can leave the cylinder tangentially in the Mach cone from the point of tangency. In general the shortest possible acoustical path from the leading edge of one wing-body juncture to a point on the opposite wing will be composed in part of a helical path on the cylinder plus a straight path. A simple calculation gives the following result for the forward boundary of the region of influence.

$$z = \left(\pi - \cos^{-1}\frac{a}{x}\right)a + \sqrt{x^2-a^2} \qquad (2)$$

The coordinate system is described in Figure (2). It is to be noted that the forward boundary parallels the Mach line of the juncture asymptotically for large x. It is significant that one of the essential

boundaries in the problem should be given by a transcendental equation. This presages the analytical difficulties inherent in the wing-body problem.

The afterbody of the combination is that part of the body lying downstream of the helices originating at the trailing edges of the wing-body junctures. In this region the effect of the wing wake will be felt on the body. In general the wing wake will be entirely non-uniform with respect to downwash. In effect, it is equivalent to a continuation of the wing with both twist and camber. If the twist and camber were known, the interference between the afterbody and the wake could be determined. In general, therefore, the afterbody interference pressure field will depend on the interference between the body and wing. The complexity of the afterbody problem is thus apparent. Only the winged section will be analyzed in detail.

2.2 Boundary Conditions

Henceforth only configurations having a vertical plane of symmetry will be considered. The question of a horizontal plane of symmetry is not important since the problems to be considered in this paper will be those for which the flow above the wing will be independent of the flow beneath the wing. This is the case when the wing leading and trailing edges are supersonic. If a subsonic

side edge exists there will usually be a tip region where interaction between the upper and lower wing surfaces is possible, but this region will only have an effect on the wing-body interference for low values of the reduced aspect ratio, $AR\sqrt{M^2-1}$. In cases where the upper and lower wing surfaces cannot interact, the symmetry conditions about the horizontal plane are unimportant. In fact if a flat rectangular wing is inclined at a degree α on a body at zero angle of attack, the pressures will be antisymmetric about the horizontal plane. If however the wing is a wedge of half-angle α at zero angle of attack on the body, then the pressures will be symmetric. It is clear that both problems are essentially the same, and it is only necessary to solve the problem for one side of the wing in either case since the solution for the other side follows from the known symmetry properties. Attention will henceforth be focused in the region above the horizontal plane through the body axis.

A decomposition of a very important class of boundary-value problems into simpler problems has been suggested by Lagerstrom and Van Dyke in Reference (9). It is assumed that the boundary conditions can be specified on a plane for the wing and on a cylinder for the body. Under these circumstances the problem of a body together with wing both inclined at different angles can be decomposed as shown in Figure (3). Although it is not necessary that either α_B or α_W be uniform, such is usually the case. In the figure the wing

has not been cut off because the effect of wing tips will not be considered. Except for very small reduced aspect ratios, the effect of wing tips is a pure wing problem. Also no nose effect has been included and the body is supposed to extend indefinitely far upstream. Neglecting the effect of the nose on wing-body interference is permissible in all but a few instances. It is to be noted that the condition (b) corresponds to the body-alone flow. In the region to be occupied by the wing there is an upwash field where the upwash varies spanwise but not chordwise. In condition (c) a twisted wing having an equal and opposite angle of attack to the upwash field has been introduced. Thus the complicated wing-body problem has been decomposed into a body-alone problem (b) plus two wing-body problems of the same type with the body at zero angle of attack and wings of the same planform but differing in twist. The twist of (c) is the negative of α_u, the upwash due to the inclined body. Neglecting the effect of the body nose, this upwash field is given by the following equation for uniform α_B:

$$\alpha_u = \alpha_B \left(1 + \frac{a^2}{x^2}\right) \tag{3}$$

At the body the upwash angle is twice the angle of attack, the angle of attack being measured from the z axis fixed in the body. The type of problem exemplified by Figures (3a) and (3c) is the kind considered in this paper. The mathematical formulation of this

type of problem is now presented.

Consider a wing-body combination such as that shown in Figure (2) subject to the condition that the wing leading edge be supersonic. Continue the wing through the body from side to side in some convenient manner and let α_B be zero. The angle of attack of the part of the wing blanketed by the body can be arbitrarily specified in any convenient manner. Let ϕ_W be the perturbation potential for the wing alone. Consider the decomposition of the problem shown in Figure (4). For $z < 0$ in the wing-alone flow field (i) the position where the cylinder would be corresponds to a streamtube. However for $z > 0$ the sidewash and downwash due to the wing alone will cause flow normal to the position the cylinder would occupy. This causes the apparent body to be somewhat distorted from the true cylindrical shape. This distortion is analogous to the apparent twist of a tailplane due to wing downwash. Since the distorted cylinder must be returned to the true cylindrical shape, an interference potential ϕ must arise. It must cancel the normal velocity induced against the body by ϕ_W and at the same time must not distort the wing shape. For the body to be a cylinder the first boundary condition is thus

$$\frac{\partial}{\partial r}(\phi_W + \phi) = 0 \; ; \; r = a \qquad (4)$$

For the interference potential ϕ not to change the wing shape the second boundary condition is

$$\frac{\partial \phi}{\partial \theta} = 0 \; ; \quad \theta = 0, \pi \tag{5}$$

where $\theta = 0, \pi$ defines the "plane of the wing". An additional boundary condition is necessary to preclude the possibility of upstream waves. These are mathematically possible because the differential equation is invariant to a change in the sign of z, and the boundary conditions specified so far do not differentiate between the plus and minus z directions. A convenient way to assure only downstream waves is to specify

$$\phi = 0 \; ; \quad z \leq 0 \tag{6}$$

From physical considerations it also follows that $\frac{\partial \phi}{\partial z} = 0$, $z \leq 0$ except possibly at the leading-edges of the wing-body junctures.

The boundary-value problem is a mixed one in that data are prescribed on time-like surfaces (Equation (4) and (5)) and a space-like surface (Equation (6)). Since the afterbody problem is not considered, the wing is taken to extend downstream indefinitely and the boundary conditions on the time-like surfaces are taken on a semi-infinite interval. This suggests the use of Laplace transform theory in the formal mathematical solution.

2.3 Formal Mathematical Solution by Laplace Transform Theory

The problem of wing-body interference explained in the preceding section can be stated in the following manner assuming, as previously mentioned, a vertical plane of symmetry.

Given: $\phi_w(r,\theta,z)$; $\Box\phi_w = 0$; $\phi_w(r,\theta,z) = \phi_w(r,\pi-\theta,z)$

Find: ϕ with $\Box\phi = 0$ such that

$$\text{(i)} \quad \frac{\partial\phi}{\partial r} = -\frac{\partial\phi_w}{\partial r} \; ; \quad r = 1$$

$$\text{(ii)} \quad \frac{\partial\phi}{\partial\theta} = 0 \; ; \quad \theta = 0, \pi \qquad (7)$$

$$\text{(iii)} \quad \phi = 0 \; ; \quad z \leq 0$$

for the range of variables $0 \leq z \leq \infty$, $0 \leq \theta \leq \pi$, $1 \leq r \leq \infty$. The radius has been taken as unity without any loss of generality.

In cylindrical coordinates the wave equation for ϕ is

$$\phi_{rr} + \frac{1}{r}\phi_r + \frac{1}{r^2}\phi_{\theta\theta} - \phi_{zz} = 0 \qquad (8)$$

Operating on each term of the equation with the Laplace operator

$$L(\;) = \int_0^\infty e^{-sz}(\;)\,dz$$

one obtains for the transformed potential Φ the partial differential equation

$$\Phi_{rr} + \frac{1}{r}\Phi_r + \frac{1}{r^2}\Phi_{\theta\theta} - s^2\Phi = 0 \qquad (9)$$

The particular solutions of Equation (9) applicable to the present problem are linear combinations formed of products of trigonometric and Bessel functions

$$\phi = \left\{ \begin{matrix} \sin m\theta \\ \cos m\theta \end{matrix} \right\} \left\{ \begin{matrix} I_m(sr) \\ K_m(sr) \end{matrix} \right\} \tag{10}$$

where the arbitrary constants are functions of s. The functions I_m and K_m are modified Bessel functions.

If the sine terms in Equation (10) are eliminated it is possible to satisfy Equation (7ii) by choosing integral values for m. Furthermore by limiting the problem to wing-body combinations with vertical planes of symmetry, the values of m are even integers. It can be shown from the asymptotic expansion that a term of Equation (10) containing $I_m(sr)$ will represent a wave traveling upstream in the direction of the characteristics z+r = constant. Although a superposition of these waves can satisfy the third boundary condition in certain instances, such a superposition is unnecessary in the present case. Only the Bessel functions $K_m(sr)$ are retained henceforth. The general form for the transformed interference potential is thus

$$\phi = \sum_{n=0}^{\infty} \phi_{2n} = \sum_{n=0}^{\infty} C_{2n}(s) \cos 2n\theta \, K_{2n}(sr) \tag{11}$$

The undetermined functions of s, $C_{2n}(s)$, are obtained by means

of the remaining boundary condition, Equation (7i).

Because of the vertical plane of symmetry, the normal velocity induced against the body by the wing can be expanded in a cosine Fourier series of even multiples of θ wherein the amplitudes are functions of z.

$$\frac{\partial \phi}{\partial r} = -\frac{\partial \phi_w}{\partial r} = \sum_{n=0}^{\infty} f_{2n}(z) \cos 2n\theta \; ; \; r=1 \tag{12}$$

With the definition

$$L\left[f_{2n}(z)\right] = F_{2n}(s) \tag{13}$$

there is obtained using Equation (11)

$$\frac{\partial \bar{\phi}}{\partial r} = \sum_{n=0}^{\infty} F_{2n}(s) \cos 2n\theta = \sum_{n=0}^{\infty} C_{2n}(s) \cos 2n\theta \; s K_{2n}'(s) \; ; \; r=1 \tag{14}$$

From this last equation the undetermined functions are finally found to be

$$C_{2n}(s) = \frac{F_{2n}(s)}{s K_{2n}'(s)} \tag{15}$$

The potential in the s-plane is

$$\bar{\phi} = \sum_{n=0}^{\infty} F_{2n}(s) \frac{K_{2n}(sr)}{s K_{2n}'(s)} \cos 2n\theta \tag{16}$$

ϕ is the inverse transform of $\bar{\phi}$, or

$$\phi = L^{-1}\left[\sum_{n=0}^{\infty} F_{2n}(s) \frac{K_{2n}(sr)}{s K_{2n}'(s)} \cos 2n\theta \right] \tag{17}$$

Assuming the existence of ϕ, Equation (17) gives the formal mathematical solution of the boundary-value problem. If ϕ were to be found in a table of Laplace transforms such as Reference (12), the problem would be solved practically as well as formally. However the possibility of finding ϕ is remote, and further manipulation of Equation (17) is required to get a practical solution. As will be pointed out, Equation (17) provides a practical method of determining the body pressures, but for a general point in the field a different approach is more convenient. The new approach, adapted to numerical work, is simply a different mathematical formulation of the problem leading, of course, to the same results as the Laplace transform theory.

2.4 Formal Solution by Method of Axial Distributions

In the foregoing section it was shown that the interference perturbation velocity potential ϕ could be determined as a superposition of potentials varying as $\cos 2n\theta$. Each of these potentials can be interpreted as that for a wing-body combination, the one corresponding to $n = 0$ being axially symmetric. These wing-body combinations when added together will produce condition (ii) of Figure (4). Thus the wing-body combinations will correct the distortion of the cylindrical body caused by the wing-alone pressure field. Each of these wing-body combinations would appear to be

quasi-cylindrical. However since the boundary conditions are to be applied on the cylinder, the problem is exactly cylindrical. For n = 0 $\cos 2n\theta$ is unity, and the wing-body combination for this case is axially symmetric. The geometry of the configuration is shown in Figure (5). The normal velocity at the cylindrical surface, the pressure coefficients, and the potential all have no dependence on θ. For n = 1 the corresponding properties of the wing-body combination vary as $\cos 2\theta$. Figure (5) also illustrates this condition. It is to be noted however that the amplitudes of the normal velocities and pressures vary in the downstream direction.

Karman and Moore in Reference (10) have given a method of determining the pressure field of an axially symmetric body at zero angle of attack by distributing along the axis of the body a certain fundamental solution in such strength as to satisfy the boundary conditions at the body surface. It is significant to ask whether or not it is possible to determine the potential and pressure fields of the wing-body combinations for $n > 0$ by means similar to those of Karman and Moore. The question can be answered in the affirmative. The method depends on using a suitable fundamental solution.

The fundamental solutions sought are of the type varying as $\cos 2n\theta$ and are thus of the form $h_{2n}(z,r)\cos 2n\theta$ where $h_{2n}(z,r)$ is a function of z and r. The only condition on h(z,r) is given by

Equation (7iii) since (7ii) is satisfied as before and Equation (7i) is satisfied by distributing the fundamental solution in variable strength along the axis. It is known that functions of the form $(z^2-r^2)^{\frac{m}{2}}$ where m is a positive odd integer will be imaginary outside the downstream Mach cone from the origin and hence will have no real contribution to the potential there. If now $h_{2n}(z,r)\cos 2n\theta$ is substituted into the wave equation in cylindrical coordinates, the function $h_{2n}(z,r)$ will be found to obey the differential equation

$$\frac{\partial^2 h_{2n}}{\partial r^2} + \frac{1}{r}\frac{\partial h_{2n}}{\partial r} - \frac{4n^2}{r^2}h_{2n} - \frac{\partial^2 h_{2n}}{\partial z^2} = 0 \qquad (18)$$

Particular solutions of Equation (18) containing a factor of the type $(z^2-r^2)^{\frac{m}{2}}$ are given as

$$h_{2n}(z,r) = \frac{(z^2-r^2)^{2n-1/2}}{r^{2n}} \qquad \text{(i)}$$

$$h_{2n}(z,r) = \frac{r^{2n}}{(z^2-r^2)^{2n+1/2}} \qquad \text{(ii)} \qquad (19)$$

Although either set of fundamental solutions should be feasible, the second set has a high order singularity on the Mach cone. It is the first set that is directly related to the Laplace transform solutions. Derivatives of $h_{2n}(z,r)\cos 2n\theta$ with respect either to z or θ will be possible fundamental solutions. It now remains to be shown that these solutions can be distributed along the axis

to satisfy Equation (7i).

Consider a point P as shown in Figure (6). The potential $\phi_{2n}(P)$ associated with the n'th Fourier component is

$$\phi_{2n}(P) = \frac{\cos 2n\theta}{r^{2n}} \int_{-1}^{z-r} g_{2n}^*(\xi) \left[(z-\xi)^2 - r^2\right]^{2n-1/2} d\xi \tag{20}$$

where $g_{2n}^*(\xi)$ is the strength function for the axial distribution of the fundamental solution. It is apparent that determining $g_{2n}^*(\xi)$ is tantamount to finding $\phi_{2n}(P)$ anywhere in the field, presuming the existence of $g_{2n}^*(\xi)$. Before proceeding it is convenient to change the limits of the integral by introducing the change

$$g_{2n}(\xi) = g_{2n}^*(\xi - 1) \tag{21}$$

so that Equation (20) becomes

$$\phi_{2n}(P) = \frac{\cos 2n\theta}{r^{2n}} \int_{0}^{z-r+1} g_{2n}(\xi) \left[(z-\xi+1)^2 - r^2\right]^{2n-1/2} d\xi \tag{22}$$

By differentiation one obtains

$$\left.\frac{\partial \phi_{2n}}{\partial z}\right|_{r=1} = \cos 2n\theta \frac{\partial}{\partial z} \int_{0}^{z} g_{2n}(\xi) \left[(z-\xi+1)^2 - 1\right]^{2n-1/2} d\xi \tag{23}$$

Equation (23) is a Volterra integral equation of the first kind with a kernel of the type $K^*(z-\xi)$. Assuming that the properties of $g_{2n}(\xi)$ are such that the integrand is zero at the variable upper limit where the kernel is zero (except for n = 0) there is obtained

$$\left.\frac{\partial \phi}{\partial z}\right|_{r=1} = \cos 2n\theta \int_{0}^{z} g_{2n}(\xi) \frac{\partial}{\partial z} \left[(z-\xi+1)^2 - 1\right]^{2n-1/2} d\xi \; ; \; n \neq 0 \tag{24}$$

There is a simple relationship between the components of the integral equation as follows:

$$\mathcal{L}\left[\left.\frac{\partial \phi_{2n}}{\partial z}\right|_{r=1}\right] = \cos 2n\theta\, \mathcal{L}[g_{2n}]\,\mathcal{L}[K^*] \qquad (25)$$

where $K^*(z-\xi) = \frac{\partial}{\partial z}\left[(z-\xi+1)^2-1\right]^{2n-1/2}$

From the point of view of Laplace transform theory, Equation (24) is simply the convolution integral corresponding to Equation (25). This simple duality between Volterra integral equations of the first kind with the type of kernel discussed here and Laplace transform theory supplies the formal connection between the two methods used herein to solve the wing-body interference problem. There is complete one-to-one correspondence between the Fourier components of each method.

Now in the preceding section it was found (Equation (17)) that

$$\mathcal{L}\left(\frac{\partial \phi_{2n}}{\partial z}\right) = \cos 2n\theta\, F_{2n}(s)\,\frac{K_{2n}(s)}{K_{2n}'(s)}\;;\; r=1 \qquad (26)$$

Noting (Reference (13)) that

$$\mathcal{L}[K^*(z)] = \mathcal{L}\left[\frac{\partial}{\partial z}(z^2+2z)^{2n-1/2}\right] = \frac{s\,\Gamma(2n+1/2)\,e^s K_{2n}(s)}{\sqrt{\pi}\,(s/2)^{2n}} \qquad (27)$$

Equations (25), (26) and (27) yield

$$G_{2n}(s) = 2^{2n}\frac{(2n.!)}{(4n.!)}\,F_{2n}(s)\,\frac{s^{2n-1}}{e^s K_{2n}'(s)} \qquad (28)$$

The inverse transform of the right-hand side of Equation (28) if it

were known would be the strength being sought. Now the inverse transform $f_{2n}(z)$ of $F_{2n}(s)$ is known and if the inverse transform of $s^{2n-1}/e^{s} K_{2n}'(s)$ existed and were known, a simple convolution based on Equation (28) could be set up to determine $g_{2n}(z)$. However if the complex inversion integral of the Laplace transform theory is applied to this function, it can readily be seen from the asymptotic form of the integrand that the integral is divergent. To overcome this difficulty, recourse is had to integration by parts.

Let $$g_{2n}^{(n+1)}(\xi) = \int_0^{\xi} g_{2n}^{(n)}(\tau)\, d\tau$$

with $$g_{2n}(\xi) = g_{2n}^{(0)}(\xi)$$

and perform 2n-1 integrations by parts of Equation (22). This yields

$$\phi_{2n}(P) = -\frac{\cos 2n\theta}{r^{2n}} \int_0^{z-r+1} g_{2n}^{(2n-1)}(\xi) \frac{\partial^{2n-1}}{\partial \xi^{2n-1}} \left[(z-\xi+1)^2 - r^2\right]^{2n-1/2} d\xi \quad (29)$$

Note that we could have started with this equation since physically it represents the superposition along the axis of fundamental solutions which are 2n-1 derivatives of the original fundamental solutions. A simple convolution integral can now be obtained for $g_{2n}^{(2n-1)}(z)$. Note also that 2n-1 differentiations amounts to one integration for the case n = 0 so that the aforementioned difficulty for this case is overcome. In a manner similar to that used to obtain Equation (28), there is obtained

$$L\left[g_{2n}^{(2n-1)}(\xi)\right] = G_{2n}^{(2n-1)}(s) = \frac{2^{2n}(2n!)}{(4n!)} \left[s F_{2n}(s)\right]\left[s e^{s} K_{2n}'(s)\right] \quad (30)$$

This is the equation that has been used to determine the axial strength distributions. The convolution integral for $g_{2n}^{(2n-1)}(z)$ will now be found.

The inverse transform of the quantity $sF_{2n}(s)$ is known from the given information.

$$\mathcal{L}^{-1}[s F_{2n}(s)] = f_{2n}'(z) \tag{31}$$

However the inverse transform of the second factor in Equation (30) defines a hitherto untabulated function

$$M_{2n}(z) \equiv \mathcal{L}^{-1}\left\{\frac{1}{s e^{s} K_{2n}'(s)}\right\} \tag{32}$$

The $M_{2n}(z)$ functions will subsequently be developed in detail. The convolution integral corresponding to Equation (30) can now be formed.

$$g_{2n}^{(2n-1)}(z) = 2^{2n}\frac{(2n.!)}{(4n.!)}\int_0^z f_{2n}'(\xi) M_{2n}(z-\xi)\,d\xi \tag{33}$$

The particular virtue of Equation (33) is that it gives the axial strength function as a simple integral of a function known from the boundary conditions together with a characteristic function independent of the boundary conditions. Once the strength function $g_{2n}^{(2n-1)}(z)$ has been determined, the interference potential (or pressure) can be determined from Equation (29) for any point in the field. This solves the boundary-value problem. Before discussing in detail the $M_{2n}(z)$ functions, some discussion of pressure coefficient determination will be given.

2.5 Determination of the Pressure Coefficients

The pressure coefficient is defined as

$$C_p = \frac{p - p_0}{\frac{1}{2} \rho V_0^2}$$

and on the basis of linear theory is given by

$$C_p = \frac{-2 \, \partial \phi / \partial z}{V_0} \tag{34}$$

Using this result together with Equation (29) yields

$$C_{p_{2n}} = -\frac{2 \cos 2n\theta}{V_0 \, r^{2n}} \int_0^{z-r+1} g_{2n}^{(2n-1)}(\xi) \frac{\partial^{2n}}{\partial \xi^{2n}} \left[(z - \xi + 1)^2 - r^2 \right]^{2n-1/2} d\xi \tag{35}$$

2.6 Alternate Method of Obtaining Body Pressure Coefficient

In the methods already described it was shown that by determining first the function $g_{2n}^{(2n-1)}(\xi)$ for the desired Fourier component that the potential or pressure anywhere in the flow field can be obtained. It is possible to go directly from the boundary conditions to the pressure coefficient on the body if another set of characteristic functions is introduced. Consider the interference potential given by Equation (17)

$$\phi_{2n} = \cos 2n\theta \, \mathcal{L}^{-1} \left[F_{2n}(s) \frac{K_{2n}(sr)}{s \, K'_{2n}(s)} \right] \tag{36}$$

From Equation (34) and the relationship

$$\mathcal{L} \left(\frac{\partial \phi_{2n}}{\partial z} \right) = -s \, \mathcal{L} \phi_{2n} \tag{37}$$

it follows readily that

$$C_{p_{2n}} = \frac{2\cos 2n\theta}{V_o}\left\{ L^{-1}F_{2n}(s) - L^{-1}\left[\frac{F_{2n}(s)\left(K_{2n}(s) + K_{2n}'(s)\right)}{K_{2n}'(s)} \right] \right\} \quad (38)$$

Let the inverse transform of the expression involving the Bessel function be taken as the definition of a set of characteristic functions.

$$W_{2n}(z) \equiv L^{-1}\left[\frac{K_{2n}(s) + K_{2n}'(s)}{K_{2n}'(s)} \right] \quad (39)$$

Then the equation for the body pressure coefficient given by Equation (38) becomes

$$C_{p_{2n}} = \frac{2 f_{2n}(z)\cos 2n\theta}{V_o} - \frac{2\cos 2n\theta}{V_o}\int_0^z f_{2n}(\xi) W_{2n}(z-\xi)\, d\xi \quad (40)$$

It will be shown subsequently that the first term represents the effect of the disturbance right at the point (the so-called Ackeret value) while the second term represents the accumulated effect of all other points suitably weighted in proportion to their influence. In this connection the $W_{2n}(z)$ functions have a very simple physical significance.

The $W_o(z)$ function has been investigated by G. N. Ward in his paper on quasi-cylindrical flow, Reference (14), and it is the symbol of Ward that has been adopted here. The $W_{2n}(z)$ functions have interesting mathematical and physical properties and will be discussed later.

It has been shown that the pressure anywhere on the body

due to any Fourier component can be evaluated as the simple integral given by Equation (40). The question arises as to whether or not this direct method cannot be used to determine wing pressures. Unfortunately while one set of characteristic functions is ample for determining the body pressures, a separate set would be required for each spanwise position on the wing. It thus seems better to proceed to the axial strength function through one set of characteristic functions, and hence to the pressure at any point on the wing.

III. PROPERTIES OF THE CHARACTERISTIC FUNCTIONS

3.1 Determination of $M_{2n}(z)$ Functions

The $M_{2n}(z)$ functions have been defined as the inverse transform of an expression involving the modified Bessel functions of the second kind in accordance with the following equation:

$$M_{2n}(z) \equiv L^{-1}\left[\frac{1}{s e^{s} K_{2n}'(s)}\right] \tag{41}$$

From this definition a Fourier integral representation for $M_{2n}(z)$ will be obtained with the help of the complex inversion formula of Laplace transform theory. It will be noted that the expression on the right hand side of Equation (41) exhibits singularities at the origin and at the zeros of $K_{2n}'(s)$, which are all in the left half-plane. The contour shown in Figure (7) is to the right of all the singularities and is the one used with the complex inversion formula (Reference (15)).

$$M_{2n}(z) = \frac{1}{2\pi i}\int_{-i\infty}^{i\infty} \frac{e^{sz}}{s e^{s} K_{2n}'(s)}\, ds \tag{42}$$

Since there are no singularities of the function in the region bounded by the contour of Equation (42) and a large semi-circle in the right half-plane, by Cauchy's theorem the integral could be alternately integrated over this semi-circle. Using the asymptotic expansion for $K_{2n}'(s)$ as given in Reference (16), the asymptotic form of the integrand is

$$\frac{e^{-sz}}{-s\,e^{-s}K'_{2n}(s)} \sim -\sqrt{\frac{2}{\pi}}\;\frac{e^{-sz}}{\sqrt{s}}\left[1+O\left(\frac{1}{s}\right)\right] \tag{43}$$

If $R/z<0$ it is clear that the exponential dominant of the integrand will make the integral over the semi-circle not only absolutely convergent but convergent to zero. Therefore

$$M_{2n}(z)=0 \quad ; \quad R/z<0 \tag{44}$$

This fact is helpful in evaluating $M_{2n}(z)$ for positive real values of z.

The conversion of Equation (42) into a Fourier integral is accomplished by a quarter revolution of the complex s plane into the complex t plane.

$$t = is \tag{45}$$

It is readily shown that the contribution of the indentation to the integral is nil, and passing to the limit of zero on the contour radius gives

$$M_{2n}(z) = -\frac{1}{2\pi i}\int_0^{\infty}\frac{e^{-it(z-1)}}{t\,K'_{2n}(-it)}\,dt + \frac{1}{2\pi i}\int_0^{-\infty}\frac{e^{-it(z-1)}}{t\,K'_{2n}(-it)}\,dt \tag{46}$$

Making use of the following identities from Reference (17),

$$K'_{2n}(it) = \frac{\pi}{2}(-1)^n\left[-J'_{2n}(t)+iY'_{2n}(t)\right]$$

$$K'_{2n}(-it) = \frac{\pi}{2}(-1)^n\left[-J'_{2n}(t)-iY'_{2n}(t)\right]$$

and rationalizing the integrands, one obtains the $M_{2n}(z)$ function as a sum of a Fourier sine transform and Fourier cosine transform.

(i) $$M_{2n}(z) = S(z) + C(z)$$

(ii) $$S(z) = \frac{2(-1)^{n-1}}{\pi^2} \int_0^\infty \frac{[J'_{2n}(t)\cos t + Y'_{2n}(t)\sin t]}{t[Y'^2_{2n}(t) + J'^2_{2n}(t)]} \sin zt\, dt$$

(iii) $$C(z) = \frac{2(-1)^{n-1}}{\pi^2} \int_0^\infty \frac{[Y'_{2n}(t)\cos t - J'_{2n}(t)\sin t]}{t[Y'^2_{2n}(t) + J'^2_{2n}(t)]} \cos zt\, dt$$

From the simple symmetry properties of the sine and cosine transforms it readily follows that

$$M_{2n}(z) = 2C(z) = 2S(z)$$

The cosine transform was used to determine $M_{2n}(z)$.

$$M_{2n}(z) = -\frac{4(-1)^n}{\pi^2} \int_0^\infty \frac{[Y'_{2n}(t)\cos t - J'_{2n}(t)\sin t]}{t[Y'^2_{2n}(t) + J'^2_{2n}(t)]} \cos zt\, dt \quad (47)$$

Ordinarily the calculation of a function from a Fourier integral is not convenient because of the infinite interval of integration unless the integrand rapidly becomes negligible or asymptotic to an integrable function. The second case was encountered for $M_{2n}(z)$. The integral is split into a finite range plus an infinite range where the asymptotic integrand is used. A sharp estimate of the error due to substituting the asymptotic integrand was found.

Denoting the part of the integrand independent of the trigono-

metric function by $I_{2n}(t)$, Equation (47) can be split up.

$$M_{2n}(z) = -\frac{4(-1)^n}{\pi^2}\left[\int_0^\tau I_{2n}(t)\cos zt\,dt + \int_\tau^\infty I_{2n}(t)\cos zt\,dt\right] \quad (48)$$

The evaluation over the finite interval is simple. The asymptotic form to be used for $I_{2n}(t)$ in the second integral is obtained with the help of the usual asymptotic expansions for the Bessel function of the first kind.

$$I_{2n}(t) \sim \frac{(-1)^n}{2}\sqrt{\frac{\pi}{t}}\left[C_0 + \frac{C_1}{(2t)} + \frac{C_2}{(2t)^2} + \cdots\right] \quad (49)$$

with

$$\text{(i)} \quad C_0 = 1.0$$

$$\text{(ii)} \quad C_1 = \frac{16n^2+3}{4}$$

$$\text{(iii)} \quad C_2 = -\frac{(16n^2-1)^2+32}{32} \quad (50)$$

$$\text{(iv)} \quad C_3 = -\frac{4096n^6 - 5888n^4 - 5456n^2 + 737}{384}$$

$$\text{(v)} \quad C_4 = \frac{65{,}536n^8 - 278{,}528n^6 - 178{,}688n^4 - 367{,}680n^2 + 29{,}889}{6144}$$

The second integral can be estimated with the help of Equation (49) as

$$\int_\tau^\infty I_{2n}(t)\cos zt\,dt = \frac{(-1)^n}{2}\sqrt{\pi}\sum_{r=0}^{m}\int_\tau^\infty \frac{\cos zt\; C_r}{\sqrt{t}\,(2t)^r}\,dt + E(n,m) \quad (51)$$

where E depends on the order of the function (n), the number of terms of the asymptotic expansion (m), the upper limit of the finite

range of integration (τ) , and the argument of the function (z). An upper bound on E will be given. The integrals involved in Equation (51) can all be reduced to integrals of either Fresnel type as tabulated in Reference (16).

In estimating the error E, it is first noted that for large t the integrand I(t) becomes a monotonic decreasing function approaching zero asymptotically. Also the difference between $I_{2n}(t)$ and the first m terms of the asymptotic expansion decreases as t increases as shown in Figure (8). The exact expression for the error is

$$E(n,m,\tau,z)=\int_{\tau}^{\infty}\left[I_{2n}(t)-\frac{(-1)^n}{2}\sqrt{\frac{\pi}{t}}\sum_{r=0}^{m}\frac{C_r}{(2t)^r}\right]\cos zt\,dt \qquad (52)$$

wherein the amplitude of the cosine wave is progressively decreasing. Since cos zt alternates regularly, the integral can be represented by an infinite series of alternating sign and is less in sum than the first term. Therefore

$$|E(n,m,\tau,z)| < \left|I_{2n}(\tau)-\frac{(-1)^n}{2}\sqrt{\frac{\pi}{\tau}}\sum_{r=0}^{m}\frac{C_r}{(2\tau)^r}\right|\int_{\tau}^{\tau+\frac{\pi}{z}}|\cos zt|\,dt$$

$$< \frac{2}{z}\left|I_{2n}(\tau)-\frac{(-1)^n}{2}\sqrt{\frac{\pi}{\tau}}\sum_{r=0}^{m}\frac{C_r}{(2\tau)^r}\right| \qquad (53)$$

This estimate gives a sharp and practical upper bound on the error involved by replacing $I_{2n}(t)$ by the first m terms of the asymptotic expansion. In the calculations the error was held to approximately

10^{-3} or less throughout.

Certain observations concerning the error are clear. The error decreases as τ or m increases, but increases as z decreases. Since the coefficients C_r increase as n increases, it is clear that more terms of the asymptotic series are required for a given accuracy as the order of the function increases.

3.2 Properties of $M_{2n}(z)$ Functions

Various properties of the $M_{2n}(z)$ functions can be obtained by the methods of Laplace transform theory. Expressions valid for small and large values of the argument can be obtained, and the integral equation defining $M_{2n}(z)$ can be obtained.

It is easily seen that the upper bound on the error as given by Equation (53) is of little value for small values of z. In fact for values of z much less than 0.1, the foregoing scheme of calculation is impractical. This is a direct consequence of the fact that the $M_{2n}(z)$ functions have a square root infinity at the origin. For the purpose of obtaining $M_{2n}(z)$ about the origin, an expansion has been used. In obtaining this expansion the asymptotic form of the transform of $M_{2n}(z)$ is determined, and from this the desired expansion is obtained. With the definition

$$M_{2n}(z) = L^{-1}\left[\frac{1}{s e^{s} K_{2n}'(s)}\right] \tag{54}$$

it is desired first to obtain the asymptotic series for the right-

hand side. This is accomplished from known properties of the Bessel functions.

$$K'_{2n}(\Delta) = -\frac{2n}{\Delta} K_{2n} - K_{2n-1} \tag{55}$$

$$e^{\Delta} K_m(\Delta) \sim \sqrt{\frac{\pi}{2\Delta}} \left[1 + \sum_{r=1}^{\infty} \frac{(4m^2-1)(4m^2-3^2)\cdots(4m^2-(2r-1)^2)}{r!\,(8\Delta)^r} \right] \tag{56}$$

The desired asymptotic series is

$$\frac{1}{\Delta e^{\Delta} K'_{2n}(\Delta)} \sim -\sqrt{\frac{2}{\pi\Delta}} \left[1 - \frac{(16n^2+3)}{1!\,(8\Delta)} + \frac{256n^4-32n^2+33}{2!\,(8\Delta)^2} - \cdots \right] \tag{57}$$

Obtaining the expansion of $M_{2n}(z)$ about the origin is equivalent to taking the inverse transform of Equation (57) term by term with the result

$$M_{2n}(z) \approx -\frac{\sqrt{2}}{\pi} \left\{ \frac{1}{\sqrt{z}} - \frac{(16n^2+3)}{4}\sqrt{z} + \frac{256n^4-32n^2+33}{96} z^{3/2} \right.$$
$$\left. - \frac{4096n^6-5888n^4+5616n^2+757}{5760} z^{5/2} + \left[\frac{65{,}536n^8+434{,}176n^6-12{,}288n^4}{-203{,}168n^2+30{,}009} \right] z^{7/2} - \cdots \right\} \tag{58}$$
$$645{,}120$$

It is readily apparent that the larger the order of the function, the more terms needed for a desired accuracy. Because of algebraic complications it was not possible to deduce readily the general form of the n'th term of the series. It is believed that the radius of convergence of the series is greater than zero, particularly as the values determined by it are in agreement with those calculated by the computation technique in the transition region.

An attempt was made to determine an asymptotic series for $M_{2n}(z)$. In cases where the transform has a simple expansion about the origin, an asymptotic expansion for the original function can be obtained (Reference (17)). However the expansion about the origin of the modified Bessel function of the second kind is extremely complicated involving products of the powers of z and powers of log z. As a result only one asymptotic term was determined. The following expansions about the origin were used.

$$K_0'(s) \sim -\frac{1}{s} + \cdots - s/2 \log s/2 + \cdots \tag{59}$$

$$K_{2n}'(s) \sim -\frac{(2n!)}{4}\left(\frac{s}{2}\right)^{-2n-1} + \cdots - \frac{n(s/2)^{2n-1}}{(2n!)} \log s/2 + \cdots \tag{60}$$

Only the log terms are significant.

These results together with the results given in Reference (17) yield the asymptotic term for the $M_{2n}(z)$ functions.

$$M_0(z) \sim -\frac{1}{z^3} \tag{61}$$

$$M_{2n}(z) \sim -\frac{16n(6n!)}{(2n!)\,2^{6n+1}}\,\frac{1}{z^{6n+1}} \tag{62}$$

For values of z of about 4 the asymptotic term for $M_o(z)$ gives good accuracy. However for the higher order functions the results are of little value since the value of the function is negligible by the time the asymptotic term is accurate. The integral equation for

the $M_{2n}(z)$ functions is complicated and singular, and is of little interest.

The numerical values of the $M_{2n}(z)$ functions are presented in Table I, wherein the increments of the argument are chosen solely with a view to being able to plot a graph of the function. The error of the function is about .002 in the worse instances, being generally considerably less. For small values of the argument the result of Equation (58) should be used.

A physical explanation of the $M_{2n}(z)$ functions should make them more tangible. Consider for a moment the equality of Equation (33).

$$g_{2n}^{(2n-1)}(z) = 2^{2n}\frac{(2n!)}{(4n!)}\int_0^z f_{2n}'(z-\xi)\,M_{2n}(\xi)\,d\xi \tag{63}$$

Let
$$f_{2n}'(z-\xi) = 0\,; \quad z \neq \xi \tag{64}$$

and

$$\int_0^\infty f_{2n}'(\xi)\,d\xi = 1 \tag{65}$$

such that $f_{2n}'(\xi)$ is a Dirac delta function and $f_{2n}(\xi)$ is a unit step function. Then

$$g_{2n}^{(2n-1)}(z) = 2^{2n}\frac{(2n!)}{(4n!)}\,M_{2n}(z) \tag{66}$$

Thus $M_{2n}(z)$ is the axial distribution of fundamental solution necessary to produce a step in $f_{2n}(z)$, the amplitude function.

3.3 Determination of $W_{2n}(z)$ Functions

The determination of the $W_{2n}(z)$ function was carried out in a manner very similar to that for the $M_{2n}(z)$ functions. Formally the $W_{2n}(z)$ functions are defined as

$$W_{2n}(z) \equiv L^{-1}\left[\frac{K_{2n}(s) + K_{2n}'(s)}{K_{2n}'(s)} \right] \tag{67}$$

The function $W_o(z)$ was presented by G. N. Ward in Reference (14). The actual values of $W_o(z)$ were obtained by the Admiralty Computing Service as the byproduct of the numerical solution of some integral equations (Reference (18)).

For the application of the complex inversion formula to the determination of $W_{2n}(z)$ consider Figure (7). The formula is

$$W_{2n}(z) = \frac{1}{2\pi i} \int_{-i\infty}^{i\infty} e^{sz} \left[\frac{K_{2n}(s) + K_{2n}'(s)}{K_{2n}'(s)} \right] ds \tag{68}$$

From the asymptotic form of the $K_{2n}(z)$ functions it is readily shown that

$$\frac{K_{2n}(s) + K_{2n}'(s)}{K_{2n}'(s)} = o\left(\frac{1}{s}\right) \; ; \; |s| \to \infty \tag{69}$$

so that if z is negative and real, the integral of Equation (68) over the semi-circle of Figure (7) would be arbitrarily small as the radius becomes large. Therefore

$$W_{2n}(z) = 0 \; ; \; z < 0 \tag{70}$$

Again the conversion of the integral of Equation (68) into a Fourier integral is accomplished by a quarter revolution of the s plane into the t plane in accordance with Equation (45). However it is first shown that the indentation of the original contour about the singularity at the origin produces no contribution as the indentation shrinks to zero radius. Around the origin the integrand has the following approximate form:

$$e^{\Delta z}\frac{[K_{2n}(\Delta)+K_{2n}'(\Delta)]}{K_{2n}'(\Delta)} \approx \frac{\frac{1}{2}\left(\frac{\Delta}{2}\right)^{-2n}(2n-1)! - \frac{1}{4}\left(\frac{\Delta}{2}\right)^{-(2n+1)}(2n)!}{-\frac{1}{4}\left(\frac{\Delta}{2}\right)^{-2n-1}(2n)!} \quad ; n \neq 0 \tag{71}$$

$$e^{\Delta z}\left[\frac{K_0(\Delta)+K_0'(\Delta)}{K_0'(\Delta)}\right] \approx -\frac{\log\Delta - 1/\Delta}{-\frac{1}{\Delta}} \tag{72}$$

It follows that the contribution of the indentation is zero in the limit.

The quarter revolution of the s plane into the t plane converts the modified Bessel functions into Hankel functions as follows:

$$K_m(ze^{\pm i\frac{\pi}{2}}) = \pm\frac{\pi i}{2}e^{\mp\frac{m\pi i}{2}}\left[-J_m(z) \pm iY_m(z)\right] \tag{73}$$

Under the transformation Equation (68) yields

$$W_{2n}(z) = \frac{1}{2\pi}\int_0^\infty e^{itz}\left[\frac{K_{2n}'(it)+K_{2n}'(it)}{K_{2n}'(it)}\right]dt + \frac{1}{2\pi}\int_0^\infty e^{-itz}\left[\frac{K_{2n}(-it)+K_{2n}'(-it)}{K_{2n}'(-it)}\right]dt \tag{74}$$

When use is made of Equation (73), and the resulting integrals are separated into real and imaginary parts, only the real part remains

$$W_{2n}(z) = 2\,C^{*}(z) = 2\,S^{*}(z) \tag{75}$$

$$C^{*}(z) = \frac{1}{\pi}\int_{0}^{\infty}\left[1 - \frac{2/\pi t}{J_{2n}'^{2}(t) + Y_{2n}'^{2}(t)}\right]\cos zt\,dt \tag{76}$$

$$S^{*}(z) = -\frac{1}{\pi}\int_{0}^{\infty}\left[\frac{Y_{2n}(t)\,Y_{2n}'(t) + J_{2n}(t)\,J_{2n}'(t)}{J_{2n}'^{2}(t) + Y_{2n}'^{2}(t)}\right]\sin zt\,dt \tag{77}$$

For purposes of computation either the sine or cosine transform can be used, although use was actually made of the cosine transform. The numerical determination of the $W_{2n}(z)$ functions was carried out in a manner similar to that for the $M_{2n}(z)$ functions.

$$W_{2n}(z) = \frac{2}{\pi}\int_{0}^{\tau} I_{2n}^{*}(t)\cos zt\,dt + \frac{2}{\pi}\int_{\tau}^{\infty} I_{2n}(t)\cos zt\,dt \tag{78}$$

with

$$I_{2n}^{*}(t) = 1 - \frac{2/\pi t}{J_{2n}'^{2}(t) + Y_{2n}'^{2}(t)} \tag{79}$$

The asymptotic expression used for the integrand is

$$I_{2n}^{*}(t) = \frac{C_2^{*}}{(2t)^2} + \frac{C_4^{*}}{(2t)^4} + \cdots \tag{80}$$

with

$$C_2^* = -(8n^2 - 3/2)$$

$$C_4^* = -(96n^4 - 116n^2 + 63/8) \tag{81}$$

The second integral of Equation (78) evaluated by means of the asymptotic series is

$$\int_\tau^\infty I_{2n}^*(t)\cos zt\,dt = \sum_{r=0}^{m} C_{2n}^* \int_\tau^\infty \frac{\cos zt}{(2t)^r}\,dt + E^*(n,m) \tag{82}$$

The integrals involved in Equation (82) reduce either to S_i' or C_i' integrals instead of Fresnel integrals. The numerical values of these, both from Reference (19), were used in the computation. Again the error E* was easily estimated and the magnitude was held to about 10^{-3}.

3.4 Properties of $W_{2n}(z)$ Functions

In the study of the mathematical properties of the $W_{2n}(z)$ functions, their expansions about the origin were found, and asymptotic results were obtained. Some interesting mathematical properties of the zeros of $W_{2n}(z)$ were found. Although the integral equations for $W_{2n}(z)$ were developed, no differential equation nor recurrence formula was found. A simple physical explanation of the

$W_{2n}(z)$ functions exists.

The expansion about the origin of $W_{2n}(z)$ is equivalent to taking the term by term inverse transform of $\frac{K_{2n}(s) + K'_{2n}(s)}{K'_{2n}(s)}$ in its asymptotic form. The asymptotic form is

$$\frac{K_{2n}(s) + K'_{2n}(s)}{K'_{2n}(s)} \sim \frac{1}{2}\left(\frac{1}{s}\right) + \frac{16n^2-3}{8}\left(\frac{1}{s^2}\right) + \cdots \quad (83)$$

Taking the inverse transform term by term gives for $W_{2n}(z)$ the result

$$W_\nu(z) = \frac{1}{2} + \frac{(4\nu^2-3)}{8}z - \frac{(8\nu^2-3)}{16}z^2 - \frac{(48\nu^4-232\nu^2+63)}{768}z^3 + \frac{(48\nu^4-116\nu^2+27)}{768}z^4 + \frac{336\nu^6-4856\nu^4+8725\nu^2-1899}{122,880}z^5 + \cdots \quad (84)$$

Ward in Reference (14) states that for $W_o(z)$ the expansion is the Taylor expansion with radius of convergence 2. Because of algebraic difficulties, the general term of Equation (84) was not deduced.

For reasons mentioned in connection with $M_{2n}(z)$ only one term is obtained for the asymptotic expression of $W_{2n}(z)$. The asymptotic expansion of $W_{2n}(z)$ is obtained by using the following result for the expansion about the origin of the transform.

$$\frac{K_{2n}(0)+K'_{2n}(0)}{K'_{2n}(0)} \approx 1 - \frac{s}{2n} + \frac{8}{\pi^2(2n+1)}\left(\frac{s}{2}\right)^{4n+1}\log\left(\frac{s}{2}\right) + \cdots ; \quad (85)$$
$$n \neq 0$$

In accordance with the results of Carslaw and Jaeger (Reference (17)), only the last term produces an asymptotic term.

$$W_{2n}(z) \sim \frac{8\,\Gamma(4n+2)}{\pi^2(2n+1)\,2^{4n+1}}\left(\frac{1}{z}\right)^{4n+2}; \quad n \neq 0 \tag{86}$$

$$W_0(z) \sim \frac{1}{z^2} \tag{87}$$

In general the asymptotic expressions are of little value in numerical work as the function is usually very small before they are valid.

The convolution formula that expresses the relationship between the transform of a product and the product of the transforms yields the integral equations for the $W_{2n}(z)$ functions. For $n \neq 0$, these relationships hold.

$$L\left[2nz^{2n-1/2}(z+2)^{2n-1/2} + (4n-1)z^{2n-3/2}(z+2)^{2n-3/2}\right] = -\frac{2\Gamma(2n+1/2)\,2^{2n-1}K'_{2n}(s)}{\sqrt{\pi}\,e^{-s}s^{2n-1}} \tag{88}$$

$$L\left[2nz^{2n-1/2}(z+2)^{2n-1/2} + (1-4n)z^{2n-1/2}(z+2)^{2n-3/2}\right] = -\frac{2\Gamma(2n+1/2)\,2^{2n-1}\left[K_{2n}(s)+K'_{2n}(s)\right]}{\sqrt{\pi}\,e^{-s}s^{2n-1}} \tag{89}$$

It is then an easy result of the convolution formula that

$$\int_0^z \left[2n(z-\xi)^{2n-1/2}(z-\xi+2)^{2n-1/2} + (4n-1)(z-\xi)^{2n-3/2}(z-\xi+2)^{2n-3/2}\right] W_{2n}(\xi)\,d\xi$$
$$= 2n\left[z(z+2)\right]^{2n-1/2} - (4n-1)z^{2n-1/2}(z+2)^{2n-3/2}; \quad n \neq 0 \tag{90}$$

Equation (90) is a singular Volterra integral of the first kind with $W_{2n}(\xi)$ as the unknown function. For n = 0 the equation is not true because of a divergent integral and another result must be found.

Analogous to Equation (88) and (89)

$$\mathcal{L}\left(\frac{z+1}{\sqrt{z(z+2)}}\right) = -e^{s}K_0'(s) \tag{91}$$

and $$\mathcal{L}\left(\sqrt{\frac{z}{z+2}}\right) = -e^{s}[K_0(s) + K_0'(s)] \tag{92}$$

With these results, the convolution formula gives a simpler integral equation for $W_o(z)$.

$$\int_0^z \frac{\xi+1}{\sqrt{\xi(\xi+2)}} W_0(z-\xi)\,d\xi = \sqrt{\frac{z}{z+2}} \tag{93}$$

Again the integral equation is a singular one of Volterra's first kind.

Numerical integration of Equation (90) would be an alternate way of determining the $W_{2n}(z)$ functions, and an attempt was made to compute them using this method. The Taylor series was used to obtain the first few values of the function, and the integral equation was used to extend the range of definition of the function. The cumulative effect of errors cause the process to become inaccurate after a few steps. An unsuccessful attempt was made to develop a simple stable method before recourse was had to the method of calculation already described.

The numerical values of the $W_{2n}(z)$ functions are presented in Table II. The increments of the argument were chosen with a view to constructing graphs of the functions. The error was held to about .002, being in general less. Any obvious numerical errors

were corrected, and any small errors that may remain are of sufficiently small magnitude to have no effect on the engineering accuracy of the results. For small values of the argument, the Taylor series and calculation method were in accord in the transition region. Further evidence of the correctness of the calculations is furnished by the properties exhibited by the zeros of $W_{2n}(z)$.

The zeros of the functions were equal in number to the order of the function. (Only after the last zero does the asymptotic term have any meaning). Furthermore to the accuracy of the calculations the zeros were equally spaced, but whether this is an exact mathematical fact could not be ascertained. However the equal spacings of the zeros confirm the good accuracy of the calculations.

As previously mentioned, the $W_{2n}(z)$ functions have a direct physical significance from which their overall mathematical properties can be estimated. Specifically the $W_{2n}(z)$ function can be interpreted as proportional to the body pressures produced by a unit disturbance (delta function) in the amplitude function $f_{2n}(z)$. Let

$$f_{2n}(\xi) = 0 \; ; \; \xi \neq 0 \tag{94}$$

and

$$\lim_{\varepsilon \to 0} \int_0^{\varepsilon} f_{2n}(\xi)\, d\xi = 1 \tag{95}$$

Then applying Equation (40) to a point not at the origin

$$C_{p_{2n}} = - \frac{2 \cos 2n\theta}{V_0} W_{2n}(z) \; ; \; r = 1.0 \qquad (96)$$

The statement made above follows from Equation (96). The function $W_{2n}(z-\xi)$ is thus an influence coefficient being the influence on the pressure at z of a disturbance at ξ .

Several important physical facts follow from the numerical values of $W_{2n}(z)$. The pressure amplitude on the body due to a disturbance $f_{2n}(\xi)\cos 2n\theta$ is a damped oscillation approaching zero asymptotically, passing through zero pressure precisely 2n times, and with the points of zero pressure equally spaced. The effect of a pressure disturbance for n = 0 (axially symmetric pressure disturbance) damps to about 4 percent of its maximum value a distance of seven body radii downstream, whereas for n = 5 the same damping occurs in 2 body radii. The effect of higher harmonics to damp out quickly on the body in the downstream direction is thus apparent.

IV. APPLICATION OF METHOD TO RECTANGULAR WING-BODY COMBINATION

4.1 Wing-Alone Potential

The actual non-planar system for which the interference pressure field will be calculated is that shown in Figure (3a); namely, that of a circular body at zero incidence with a flat rectangular wing at incidence α_W. The wing alone is taken to extend straight through the body from side to side, and the Mach number is taken as $\sqrt{2}$ without loss of generality so that the Mach lines will fall at forty-five degrees to the axes.

Since the wing-alone in the region of the body is assumed independent of wing-tip effects, the flow due to the wing alone is two-dimensional and will be given by Ackeret's theory (Reference (20)). The potential for the upper half plane is

$$\phi_W = V_0 z \; ; \quad y > z \tag{97}$$

$$\phi_W = V_0 z + \alpha_W V_0 (z-y) \; ; \quad y < z \tag{98}$$

where $V_0 \alpha_W (z-y)$ is the perturbation potential due to the wing. The potential causes uniform downwash and no sidewash.

4.2 Fourier Amplitudes of the Body Normal Velocity

The $f_{2n}(z)$ functions of Equation (12) must now be determined. With $y = r \sin\theta$ and $r = 1$, Equations (97) and (98) give

$$\frac{\partial \phi_W}{\partial r} = 0 \; ; \quad r = 1.0 \; ; \quad \sin\theta > z \tag{99}$$

$$\frac{\partial \phi_w}{\partial r} = -\alpha_w V_0 \sin\theta \; ; \; r=1 \; ; \; \sin\theta < z \tag{100}$$

The results are shown in Figure (9). The $f_{2n}(z)$ functions are given by the following integrals from Fourier series theory.

$$f_0(z) = \frac{2}{\pi} \int_0^{\sin^{-1} z} \alpha_w V_0 \sin\theta \, d\theta \tag{101}$$

$$f_{2n}(z) = \frac{4}{\pi} \int_0^{\sin^{-1} z} \alpha_w V_0 \sin\theta \cos 2n\theta \, d\theta \tag{102}$$

Carrying out the integration yields the specific functions for this combination.

$$f_0(z) = \frac{2 V_0 \alpha_w}{\pi} \left[1 - \sqrt{1-z^2} \right] \; ; \; z \leq 1 \tag{103}$$

$$f_0(z) = \frac{2 V_0 \alpha_w}{\pi} \; ; \; z \geq 1 \tag{104}$$

$$f_{2n}(z) = \frac{2 V_0 \alpha_w}{\pi} \left[\frac{\cos(2n-1)\psi}{(2n-1)} - \frac{\cos(2n+1)\psi}{2n+1} - \frac{2}{4n^2-1} \right] ; \quad z \leq 1 \; ; \; n \neq 0 \tag{105}$$

$$f_{2n}(z) = -\frac{4 V_0 \alpha_w}{\pi(4n^2-1)} \; ; \; z \geq 1 \; ; \; n \neq 0 \tag{106}$$

where

$$\cos\psi = \sqrt{1-z^2}$$

It is convenient that these functions are known in closed form, but where the functional forms are unobtainable, the numerical methods of harmonic analysis can be used.

For the rectangular wing there is no sidewash outside the region of influence of the wing tips, and hence there is no contribution of the sidewash to the normal velocity at the body surface. However for wings with swept leading edges this is no longer the case. The values of the Fourier amplitudes for the general case of supersonic edges are given in the Appendix. Through the use of this Appendix, the problem carried through here for a rectangular wing can be carried through for a triangular wing with supersonic leading edges.

4.3 Axial Strength Distributions

The axial strength distributions have been computed using Equation (33). For the values of $f_{2n}(z)$ given previously, the derivatives are

$$\frac{f_{2n}'(z)}{\frac{V_0 \alpha_w}{\pi}} = \frac{4z}{\sqrt{1-z^2}} \cos\left[2n \cos^{-1}\sqrt{1-z^2}\right] ; \quad z<1 \tag{107}$$

$$\frac{f_{2n}'(z)}{V_0 d/\pi} = 0 ; \quad z>1 \tag{108}$$

As long as $z < 1$ the singularity of $f_{2n}'(\xi)$ will not be manifest. However the square root singularity of $M_{2n}(z-\xi)$ will arise. The numerical integration through such simple singularities causes no difficulty (but increases the amount of work). However at $z = 1$ the singularities of $f_{2n}'(\xi)$ and $M_{2n}(z-\xi)$ come into confluence to produce a logarithmic singularity in the strength function $g_{2n}^{(2n-1)}(z)$.

It is readily shown that for values in the neighborhood of unity, the dominant part of $g_{2n}^{(2n-1)}(z)$ is

$$2^{2n}\frac{(2n!)(-1)^n}{(4n!)}\left(\frac{4}{\pi}\right)\log|1-z| \qquad (109)$$

as $z \rightarrow 1$ from either side.

The necessity of the 2n-1 integrations by parts of Equation (20) resulting in Equation (29) is now clear. If a fundamental solution of the kind given by Equation (19) had been used, the strength functionswould have had non-integrable singularities. Even after 2n-1 integration the strength function contains a singularity, fortunately integrable.

Some values of $g_{2n}^{(2n-1)}(z)$ are plotted in Figure (10). This plot shows the singularities passing through z = 1.

4.4 Pressure Distributions of Fourier Components

Obtaining the strength functions $g_{2n}^{(2n-1)}(z)$ is tantamount to getting the pressure coefficient anywhere in the field for any one of the Fourier components. Equation (35) has been used for this purpose, the integration being performed graphically.

The pressures due to all the components are finite everywhere. Although the strength function $g_{2n}^{(2n-1)}(z)$ has a logarithmic singularity, and the other part of the integrand has a square root singularity, the integral is always finite even at the confluence of the singularities. The detailed pressure distributions will be

presented under Discussion. For large values of z-r+1 and n care must be taken in the numerical integrations to get accurate pressure results near the body. In this region, where the pressure coefficients are small, the $W_{2n}(z)$ method gives more accuracy than the $M_{2n}(z)$ method for less work.

4.5 Approximate Expressions for the Pressure Coefficients for Large and Small Values of z.

It is possible to find approximate expressions for the pressure coefficients for large and small values of z. This is best accomplished by the methods of Laplace transform theory, methods already used to get expansions for $W_{2n}(z)$ and $M_{2n}(z)$ for large and small values of the argument. From the practical point of view, the method depends on being able to transform the $f_{2n}(z)$ functions to the s-plane, and being able to obtain asymptotic expansions for the transforms.

Starting with Equation (17) for the interference potential

$$\phi = L^{-1} \sum_{n=0}^{\infty} F_{2n}(s) \frac{K_{2n}(sr)}{s K'_{2n}(s)} \cos 2n\theta \qquad (110)$$

and making use of Equation (34), one obtains

$$C_{P_{2n}} = -\frac{2 \cos 2n\theta}{V_0} L^{-1}\left[\frac{F_{2n}(s) K_{2n}(sr)}{K'_{2n}(s)}\right] \qquad (111)$$

First the analytic form of $F_{2n}(s)$ is determined. The integrals of

Equations (101) and (102) are substituted into the definition of the Laplace transform

$$F_{2n}(s) = \int_0^\infty e^{-sz} f_{2n}(z)\, dz \tag{112}$$

and the order of integration is reversed. After one integration there is obtained

$$F_{2n}(s) = \frac{2\alpha_w V_0}{\pi s} \int_0^\pi e^{-s \sin\theta} \sin\theta \cos 2n\theta \, d\theta \tag{113}$$

and

$$F_0(s) = \frac{\alpha_w V_0}{\pi s} \int_0^\pi e^{-s \sin\theta} \sin\theta \, d\theta \tag{114}$$

Equations (113) and (114) are integrated by means of a single trigonometric substitution and of certain integral formulas from Watson, Reference (16),

$$J_\nu(z) = \frac{1}{\pi} \int_0^\pi \cos(\nu\theta - z \sin\theta)\, d\theta \tag{115}$$

and

$$E_\nu(z) = \frac{1}{\pi} \int_0^\pi \sin(\nu\theta - z \sin\theta)\, d\theta \tag{116}$$

Watson calls the $J_\nu(z)$ function the Anger function, which reduces to the usual Bessel function for integral values of ν. Watson calls the function $E_\nu(z)$ the Weber function, whereas Jahnke and Emde (Reference (21)) call it the Lommel-Weber function. The

integration of Equation (113) gives

$$F_{2n}(\xi) = -\frac{i\alpha_w V_0}{\xi}\left[J_{2n-1}(i\xi) - J_{2n+1}(i\xi) - iE_{2n-1}(i\xi) + iE_{2n+1}(i\xi)\right] \tag{117}$$

The functions $J_\nu(z)$ and $E_\nu(z)$ are respectively odd and even for odd integral values of ν, and obey the following recurrence relationships:

$$2J_\nu'(z) = J_{\nu-1}(z) - J_{\nu+1}(z) \tag{118}$$

$$2E_\nu'(z) = E_{\nu-1}(z) - E_{\nu+1}(z) \tag{119}$$

Equation (111) can now be written

$$C_{P2n} = +4\alpha_w \cos 2n\theta\, \mathcal{L}^{-1}\left\{\left[\frac{E_{2n}'(is)+iJ_{2n}'(is)}{s}\right]\left[\frac{K_{2n}(sr)}{K_{2n}'(s)}\right]\right\} \tag{120}$$

$$C_{P0} = 2\alpha_w \mathcal{L}^{-1}\left\{\left[\frac{E_0'(is)+iJ_0'(is)}{s}\right]\left[\frac{K_0(sr)}{K_0'(s)}\right]\right\} \tag{121}$$

Fortunately the transforms have simple asymptotic expansions for large s, and expansions for C_{P2n} for small z are readily obtained. In obtaining the asymptotic expansions, use is made of the results of Watson, Reference (16), p. 309, for the Weber function $E_\nu(z)$ and the Anger function $J_\nu(z)$. The simple asymptotic result is

$$E_{2n}'(is)+iJ_{2n}'(is) \sim -iH_{2n}'(is) + \frac{1}{\pi}\left[-\frac{2}{s^2} + \frac{6(4n^2-1)}{s^4} + \cdots\right]; \quad n \neq 0 \tag{122}$$

The Hankel function is dominated by a negative exponential in the right half plane and hence can be ignored in the expansion. With the aid of Equation (122) the entire asymptotic result can be written down.

$$\frac{\left[E_{2n}'(is)+iJ_{2n}'(is)\right]}{s}\left[\frac{K_{2n}(sr)}{K_{2n}'(s)}\right]\sim\frac{2e^{-s(r-1)}}{\pi\sqrt{r}}\left[\frac{1}{s^3}+\frac{16n^2(1-r)-(3r+1)}{8rs^4}+\cdots\right];\ n\neq 0 \tag{123}$$

Formally taking the inverse transform of Equation (123) will give a result for the pressure coefficient $C_{P_{2n}}$ that is in accord with the calculated solution. The following Laplace transforms are used.

$$L^{-1}\frac{e^{-s(r-1)}}{s^3}=\begin{cases}0; & z\leq r-1\\ \dfrac{(z-r+1)^2}{2}; & z\geq r-1\end{cases} \tag{124}$$

$$L^{-1}\frac{e^{-s(r-1)}}{s^4}=\begin{cases}0; & z\leq r-1\\ \dfrac{(z-r+1)^3}{6}; & z\geq r-1\end{cases} \tag{125}$$

The final result for the expansion of the pressure coefficient for small values of z-r+1 is

$$C_{P_{2n}}\approx\frac{8\alpha_w\cos 2n\theta}{\pi\sqrt{r}}\left\{\frac{(z-r+1)^2}{2}+\frac{\left[16n^2(1-r)-(3r+1)\right](z-r+1)^3}{48r}+\cdots\right];\ z\geq r-1;\ n\neq 0 \tag{126}$$

$$C_{P_{2n}}=0;\quad z\leq r-1;\quad n\neq 0 \tag{127}$$

For n = 0 the results must be halved.

Equations (126) and (127) disclose several interesting results. For r = 1 the first two terms are the same for all the Fourier components. This can mean only that the range of validity of the result must decrease as n increases since the pressures are in fact finite everywhere for the wing-body combination. The lines z-r+1 equal a constant correspond to the downstream characteristics, and on the basis of the first term the pressures near the origin of z damp along the characteristics inversely proportional to the square root of the radius. This phenomenon turns out to be a good approximation for a large region for n = 0, but is of little value for the higher order Fourier components. The result shows no increase in damping as n increases. It will subsequently be shown that the pressure coefficient based on Ackeret's theory is a better approximation to the true solution for small values of z on the body. However the present solution has the advantage that it predicts the mathematical form of the solution for small values of z-r+1 for points off the body as well as those on the body.

To obtain approximate values of $C_{P_{2n}}$ for large values of z, it is necessary to expand the transforms of Equations (120) and (121) about the origin. For the Fourier components of order greater than zero, it is to be expected that the asymptotic results will be

valid only after the last zero of the pressure coefficient. Only for n = 0 will the asymptotic result be of much value. One asymptotic term for $C_{P_{2n}}$ will now be given.

The first step in obtaining the asymptotic term is to expand the transform about the origin and find the first term giving an asymptotic result. This term is given as

$$\frac{F_{2n}(s)K_{2n}(sr)}{K_{2n}'(s)} : \quad \frac{8\alpha_w V_0 (r^{2n}+r^{-2n})\left(\frac{s}{2}\right)^{4n}\log s}{\pi(4n^2-1)(2n!)^2} \tag{128}$$

$$\frac{F_0(s)K_0(sr)}{K_0'(s)} : \quad \frac{2\alpha_w V_0 \log s}{\pi} \tag{129}$$

These terms produce the following asymptotic results for $C_{P_{2n}}$ with the aid of Carslaw and Jaeger, Reference (17):

$$C_{P_{2n}} \sim \frac{-32\alpha_w \cos 2n\theta\,(r^{2n}+r^{-2n})(4n!)}{\pi 2^{4n+1}(4n^2-1)(2n!)^2 z^{4n+1}} \tag{130}$$

$$C_{P_0} \sim \frac{4\alpha_w}{\pi z} \tag{131}$$

V. RESULTS AND DISCUSSION

5.1 Interference Pressure Distributions of the Fourier Components

The results presented and discussed herein are for a circular body of unit radius at zero angle of attack with an inclined flat rectangular wing. The chord of the wing is four body radii, and the span of the wing is arbitrary since no tip effects are considered.

The pressure distributions associated with the interference potential ϕ are presented in the Figures (11) to (14) for the first four Fourier components. The pressures are presented for four values of r so that the span loading curves for each Fourier component could be established. With regard to the first component for n = 0, the axially symmetric component, Figure (11) shows that it produces interference pressures of invariable sign. The abscissa has been so chosen that it measures distances behind the Mach line lying on the wing and originating at the leading edge of the wing-body juncture. The discontinuities in slope of the pressure distributions at z-r+1=1 are a consequence of the fact that the body becomes totally immersed in the wing-alone flow field at z = 1. The higher Fourier components tend to neutralize this discontinuity in slope, since the pressure distribution should be smooth here for the actual wing-body combination.

It is apparent that the pressure distribution is propagated outward from the body along the downstream characteristics and

that a damping of the pressure occurs. For small values of z-r+1, the pressure coefficients are in good accord with the approximate results of Equation (126). On the basis of this equation the pressure coefficients should vary inversely as the square root of r in the region of validity of the expansion for small z-r+1. A glance at the figure reveals this to be approximately the case even in regions where the approximate result for small z-r+1 is no longer valid. However for large values of z, the asymptotic result, Equation (131), predicts that no variation with r will occur. If the value of r is held constant, and z is increased sufficiently the pressure distribution should approach that for the wing-body juncture. Even within the range of the figure, this tendency is seen. Thus the damping of the pressure with r varies with the inverse square root of r for small values of z-r+1, to no damping for fixed r and large values of z.

Some significance can be attached to the first term of the approximate result of Equation (126) for small values of z-r+1, at least for the body. It turns out to be the first term in the series expansion for the pressure computed on the basis of the Ackeret theory of Reference (20). It is to be expected that the pressures on the body should be given accurately by Ackeret's theory for small enough values of z, since the curvature of the body will have no important effect. The domain of dependence for a

point on the body with a small z coordinate will be nearly plane, and the body normal velocity will not vary laterally because of the axial symmetry so that two-dimensional conditions are closely approximated. If the local flow angle (due to the wing-alone flow field) is α, then on the basis of Ackeret's theory

$$C_p = \frac{2\alpha}{\sqrt{M^2-1}} \tag{132}$$

For n = 0 the result given by Equation (132) is

$$C_{p_0} = \begin{cases} \frac{4\alpha_w}{\pi}\left(1-\sqrt{1-z^2}\right); & z \leq 1 \\ \frac{4\alpha_w}{\pi}; & z \geq 1 \end{cases} \tag{133}$$

This result has been incorporated into Figure (11), and the agreement between it and the true solution is very close for $z < 1$. If now the expression for C_{p_0} is expanded in a power series, the result is

$$C_{p_0} = \frac{4\alpha_w}{\pi}\left(\frac{z^2}{2} + \frac{z^4}{8} + \cdots\right) \tag{134}$$

The first term of this result is just that given by the first term of Equation (126) for r = 1. While the Ackeret value as given by Equation (133) is a better approximation than the Laplace transform result of Equation (126), it is valid only on the body and does not predict the mathematical form of the solution on the wing for small values of z-r+1.

Another significance can be attached to the Ackeret values

of the pressure coefficient as given by Equation (133). It is exactly the same as the first term in Equation (40) for calculating the pressures by means of the $W_{2n}(z)$ functions. The second term of the same equation, the convolution integral, is the cumulative effect of all the pressure disturbances in front of the point in question, and is the difference between the Ackeret value and the true value in Figure (11). It is clear that the net effect of all the non-local disturbances is sufficient to make the value of C_{P_o} approach zero as z approaches infinity, rather than the constant value the Ackeret theory predicts.

The question arises whether or not the simple asymptotic result for C_{P_o} for large z given by Equation (131) is valid. A tendency for the downstream pressures to attain this result for all the values of r is shown by Figure (11).

An examination of Figures (12), (13), and (14) for n = 1, 2, and 3 respectively, reveals a systematic variation in the pressure distributions as n increases. As n increases there is a general decrease in the magnitude of the pressure coefficients particularly for large values of z-r+1. This, of course, is necessary for convergence. A rough idea of the dependence of the magnitude of the pressure coefficients on n can be given for the body. On the basis of Equation (40) $C_{P_{2n}}$ varies directly as $f_{2n}(z)$ for large values of z since $f_{2n}(z)$ is constant for $z \gg 1$. Furthermore $f_{2n}(z)$ varies

nearly inversely as n^2 in this region with the result mentioned above. The discontinuities in the slope of the pressure distribution at values of z-r+1 of unity are still apparent, but to a lesser degree than for n = 0. The rapid oscillations in pressure near z-r+1=1 are necessary to cancel a step in pressure on the body as will be pointed out. One of the most significant changes as n increases is the increase in the number of zeros of the pressure distribution. This is a direct consequence of the nature of the characteristic functions. For instance in discussing the $W_{2n}(z)$ function it was pointed out that a unit disturbance varying as $\cos 2n\theta$ has precisely 2n zeros. The significance of the increased number of zeros is that the contributions to the span loading of the higher Fourier components will be much less proportionately than their contributions to the pressures, a fact that is of prime importance in determining the number of Fourier components that must be used.

It was hoped that the higher order Fourier components would damp faster in the characteristic directions than the Fourier components for n = 0 or n = 1, so that only very few components would be needed to obtain accurate pressure distributions on the wing away from the juncture of the wing with the body. However this effect is not of any significance. In fact the damping effect is greatest in the downstream direction rather than in the characteristic directions.

The range of validity of the results given by Equation (126) for small values of z-r+1 decreases rapidly as n increases. Figure (12) for n = 1 illustrates this point clearly when compared to Figure (11) for n = 0. The same comparison reveals that the Ackeret result for n = 1 is a good estimate of the overall trend on the body for $z < 1$, but it deviates considerably from the true solution in several places. A consideration of the boundary conditions at the body surface will explain the reason. Consider a body surface point having a small z coordinate, and focus attention on its domain of dependence on the body for $z \geq 0$. This domain of dependence is a near-plane, and if the normal velocity induced by the wing has no θ dependence, then the two-dimensional Ackeret theory will give a good approximation. However for $n > 0$, there is a dependence on θ of the normal velocity so that the plane is essentially corrugated in the θ direction. If the effect of the lateral corrugations were taken into account by using supersonic wing theory, good approximation should be obtained for values of $z < 1$ since the solution for n = 0 demonstrated that the effect of the body curvature was not very important for such small values of z.

For large values of z the asymptotic results of Equation (130) are not very significant except for n = 0. For $n > 0$, there are zeros in the pressure distribution and the value of $C_{P_{2n}}$ is very small before the asymptotic formula is valid.

5.2 Wing-Body Juncture Pressure Distribution Based on Four Fourier Components

The pressure distribution for the wing-body juncture based on four Fourier components are presented in Figure (15). From this figure a number of significant results can be obtained. The pressures due to the n = 0 and n = 1 components are large for all values of z shown in the figure. Those for n = 2 are appreciable up to about z = 3; those for n = 3 to about z = 2. This behavior illustrates that great accuracy for small values of z can be had only by increasing the number of the Fourier components, whereas good accuracy can be had for moderate values of z with relatively few components. Fortunately it is easy to obtain a good approximation for small values of z for the net effect of all the harmonics so that the necessity of taking many Fourier components is easily circumvented.

Figure (15) shows that the general effect of interference at the wing-body juncture is to reduce the magnitude of the pressure coefficients due to the wing alone. Only at z = 0 and z = ∞ is the effect of the interference nil. The reason for the behavior near z = 0 is simple. For small values of z in the juncture the body is effectively an infinite vertical wall, a perfect reflection plane. Therefore the pressure should be that for the two-dimensional rectangular wing which is identical to the wing alone. As a result the interference has zero contribution here to the pressure. As the

value of z increases there is a general decrease in the magnitude of the pressure coefficients due to the effect of interference until the pressure disturbances originating on the opposite half-wing can be felt. As discussed previously, a value of $z = \pi$ must be attained before the opposite half-wing becomes effective at the wing-body juncture. Behind this point the magnitude of the pressure coefficient is observed to increase. In fact as the rearward distance increases indefinitely the magnitude of the pressure coefficient in the juncture tends to increase to the two-dimensional value again. This effect is not unreasonable since the wing is of infinite lateral extent and the body is finite in radius for this condition. The tendency of the magnitude of the pressure to increase near $z = \pi$ is taken as an indication of the plausibility of the calculated results.

The behavior of the pressure distribution for small values of z requires clarification. Although the component pressure distributions exhibit erratic behavior near $z = 1$, the resultant pressure distribution must be smooth here since this point can be distinguished in no way for the wing-body combination. The effect is purely a result of the choice of the wing alone. Further light will be shed on this matter in connection with the discussion of the pressure distribution for the top of the combination. For small values of z more components are necessary for good accuracy, and in fact the point

z = 0 in the wing-body juncture is the focal point of convergence for the solution. Practically the solution in this region can be obtained by continuing the solution for larger z into the known value at z = 0. Better still the solution can be joined smoothly to the solution valid for small z that will now be developed.

It will be recalled that the effect of body curvature was not sufficiently great for values of $z < 1$ to cause any large differences between the true solution for n = 0 and the Ackeret solution. This suggested the use of supersonic wing theory to obtain approximate solutions in this region when the problem involved a dependence on θ. By the use of this device an approximate solution valid for small z can be obtained which represents the interference pressure distribution due to all the Fourier components. For this purpose the fundamental formula of supersonic wing theory is required.

$$\phi(x,y,z) = -\frac{1}{\pi}\iint \frac{\phi_y(\xi,0,\zeta)\, d\xi\, d\zeta}{\sqrt{(z-\zeta)^2-(y-\eta)^2-(x-\xi)^2}} \qquad (135)$$

Here φ is the potential at a point (x,y,z) due to a prescribed distribution of ϕ_y over the y = 0 plane, the integration being performed over the domain of dependence of the point. For the present wing-body combination the value of ϕ_y is sinusoidal and for sufficiently small values of z is given by

$$\phi_y = \alpha_w V_0 \xi \qquad (136)$$

in the domain of dependence shown in Figure (16). With the x,y,z axis orientation as shown in the figure

$$\phi(0,0,z) = -\frac{2\alpha_w V_0}{\pi}\int_0^{z/2}\int_{\xi}^{z-\xi}\frac{d\xi\,d\zeta}{\sqrt{(z-\xi)^2-\xi^2}} \tag{137}$$

The result for the pressure coefficient is

$$C_p = \frac{4\alpha_w z}{3\pi} \tag{138}$$

This result has been included in Figure (15), and it is clear that the net result due to four Fourier components can be smoothly joined to it.

5.3 Pressure Distribution at Top of Wing-Body Combination

The results for the pressure distribution at the top of the body are shown in Figure (17). The pressure distribution due to the wing alone has a step at z = 1. Those due to the Fourier components are essentially the same as those for the wing-body juncture except that the signs of the odd components have been reversed.

Several important effects are exhibited in Figure (17). Between z = 1 and z = $\pi/2$ the four Fourier components have essentially reduced the step in the pressure distribution due to the wing alone to zero. This is precisely what should occur from a priori considerations. It has been pointed out that for the complete wing-body combination, the effect of interference cannot be felt on the top of the body for values of z less than $\pi/2$. The step introduced at z = 1

is purely a result of the particular choice of the wing alone, and cannot occur for the real wing-body combination. If more components were calculated, it would develop that a spine near $z = 1$ would occur, but the area under the spine would decrease to zero and the spine height would approach a constant finite value as the number of harmonics increased without limit. This so-called Gibbs phenomenon is without physical importance here. This pressure distribution for $z > \pi/2$ can be joined smoothly to the value of zero at $z = \pi/2$.

The general behavior noted above is further evidence of the plausibility of the calculated results. Furthermore it sheds some light on the number of Fourier components that must be used to obtain an acceptable solution for most of the combination. At the wing-body juncture it was noted that the sum of the Fourier components must add up to a smooth function for $z = 1$. However by changing the sign of the odd components, the same components must annihilate a step in the pressure distribution at the top of the body between $z = 1$ and $z = \pi/2$. To do this with less than three or four Fourier components is clearly difficult. On the other hand these results indicate that if good results are to be obtained everywhere with one or at most two terms of some series solution, a different definition of the wing alone giving no step in the pressure distribution on the body must be used or some very clever choice of an

auxiliary solution to eliminate the step in pressure must be discovered. To find such a solution would be difficult, to say the least.

5.4 Wing Pressure Distributions

The interference pressure distributions added to the wing-alone pressure field gives the pressure distribution for the combination. In fact just this process is illustrated in Figure (15) for the wing-body juncture. The procedure and the shape of the curves is substantially the same for other wing spanwise positions. The results, which have been smoothed, are presented in Figure (18). The important effect of interference on the pressure distribution in the wing-body juncture is immediately apparent. For spanwise positions further out a lesser portion of the chord is subject to interference so that the net effect on the loading is less.

5.5 Wing-Body Combination Span Loadings

The integration of the pressure distributions already presented to obtain the span loading for any wing-body combination having particular values of chord-radius ratio and wing-alone aspect ratio can be readily accomplished. The results for the particular wing-body combination chosen in this report are interesting and illustrate several important effects. For purposes of defining the span loading the following equation is used.

$$\frac{\Delta L_{2n}}{q\alpha_w} = \int_{-s}^{s} \left\{ -\int_{0}^{\frac{c}{2}} \frac{C_{P_{2n}}}{\alpha_w} dz \right\} dx \qquad (139)$$

In this equation ΔL_{2n} is the lift on the combination up to a distance c downstream of the leading edge of the wing due to the n'th Fourier component, and $C_{P_{2n}}$ is the corresponding pressure coefficient for the upper surface. The quantity in brackets will be called the span loading. First the span loading due to the various Fourier components will be presented, and then the complete span loading for the combination will be discussed. In Figure (19) the span loadings for the various Fourier components for n = 0 to n = 2 are presented. It is emphasized that the loadings are for a downstream distance of 4 body radii and correspond to the trailing-edge location of the wing. For n = 0 a uniform pressure field exists on the body and produces a uniform loading there. However as the spanwise distance increases there is a dropping off of the loading due primarily to the decrease in the chord over which the interference pressures act. The value of r = 5 corresponds to the condition where the Mach line from the leading edge of the juncture crosses the trailing edge. Since the sign of C_{P_o} is everywhere positive, the corresponding loading is negative representing an unfavorable effect of interference on lift.

An examination of the curve of Figure (19) for n = 1 shows a very marked decrease in the span loading compared to n = 0. On the body the pressure coefficients vary as cos $2n\theta$, and this effect alone would cause a decrease in lift on the body inversely

proportional to n^2. Remembering also that the Fourier amplitudes of the normal velocity at the body surface due to the wing alone become constant at values approximately inversely proportional to n^2, it is clear that the lift on the body due to any particular harmonic should vary approximately inversely as n^4. This makes for a rapid convergence of the span loading results for the body. It should also be borne in mind that the interference span loading is only a fraction of the total lift on the combination.

With regard to the span loading on the wing of the combination, Figure (19) shows a rapid decrease in span loading as n increases. In fact for this particular case it is clear that if only one Fourier component were considered, satisfactory results would be obtained. While there is a general decrease in the overall magnitudes of the pressure coefficients $C_{P_{2n}}$ as n increases, there is another effect that is important in reducing the span loading of the higher Fourier components. This effect is the increase in the number of zeros of $C_{P_{2n}}$ as n increases. While the oscillations in $C_{P_{2n}}$ are very important in decreasing the span loading of the higher Fourier components, they are of lesser importance in reducing the contribution to the pressure distribution of the combination of the Fourier components. However it can be said on the basis of the calculated results that whereas approximately four Fourier components were necessary for good accuracy of the pressure coeffic-

ients, only one or at most two are necessary for good accuracy of the span loading.

To obtain the span loading for the combination it is necessary to consider the contributions of the body alone and the Fourier components. This has been done in Figure (20) which presents the complete combination span loading based on one Fourier component and on four Fourier components. The span loading includes no tip effects, but these can be readily introduced if desired. The contribution due to the wing-alone pressure field is the two dimensional value on the wing, but on the body there is a general loss of lift at the trailing edge position because the wing-alone pressure field cannot act on the body unless $z > \sin\theta$. (Some of this loss would be recovered on the afterbody, if any). The effect of the Fourier components is to cause a loss of loading everywhere, as the figure shows. The net result for 4 components is not greatly different than for one component, and for most practical purposes one component would have been sufficient.

The question arises as to whether the effect of interference is favorable or unfavorable for the combination, and for the body and wing. However before a satisfactory answer to this question can be given, some reference loading must be established for purposes of comparison. For this purpose two extremes have been chosen: (1) the blanketed area of the wing is supposed to act effectively at α_W and (2) the blanketed area of the wing is supposed to act

effectively at zero angle of attack. For these two extremes, two reference span loading curves can be obtained. It is noted that these two definitions correspond to the cases where the body is a perfect pressure reflecting surface, a vertical wall, and to the case where there is no reflection at the body.

A comparison of the loading curve for the combination with that based on the first definition, which corresponds to the wing alone as used here, shows that the interference is unfavorable everywhere. In fact the lift on the body is much smaller than what it would be for the blanketed area acting at α_W. This decrease is the result of two effects, the adverse geometric effect of the body in displacing the wing-alone pressure field backwards and the adverse effect of the Fourier components. The loss of lift on the wing is the result of the fact that a circular body is clearly not a perfect reflection plane as evidenced by the fact that the Fourier components cause a loss of lift.

While an interpretation of the loading for the combination with the reference loading based on the first definition shows unfavorable effects of interference, the results give an unrealistic picture since they are based on an optimistic reference loading. It is hardly to be expected that the blanket wing area will act effectively at α_W. In fact a value of $\alpha = 0$ for the blanketed area

is much closer to the aerodynamic facts. An examination of Figure (20) reveals that the reference loading based on the second definition is much closer to the true loading of the combination than that based on the first definition. The differences between the combination loading and the second reference loading can be explained on physical grounds. Consider only the wing for the moment. The combination loading is greater than the reference loading, which is based on no reflection by the body of pressure disturbances originating on the wing. The body reflects some of these disturbances back and causes an increase in wing loading. In fact a comparison of the true loading with the first reference loading, which corresponds to perfect reflection by the body, and the second reference loading which corresponds to no reflection by the body shows that the body is somewhat less than 50 percent effective as a reflector as far as the wing is concerned.

A physical explanation of the mechanism by which wing lift is carried onto the body can be given in much the same way Lagerstrom and Van Dyke in Reference (9) have discussed the carrying of lift over from the wing onto polygonal bodies. Let the wing be at positive angle of attack so that its upper surface is a source of negative pressure disturbances. These pressure disturbances are in part reflected and in part transmitted at the body. The reflected part acts to increase the wing lift. The reflected pulses must travel

upward around the body as they move downstream. In the process the pulses lose lifting potential because of a geometric effect and an aerodynamic effect. The distance around the body is further than the distance through it, and by the time the pulses reach the top of the body their lifting effect has been delayed in space and time. This geometric effect is the delayed reaction pointed out by Lagerstrom and Van Dyke. It can be offset by properly designing the afterbody. The aerodynamic effect is simply a decrease in the lifting pressure of the pulses as they travel around the body. This causes a further loss of loading at the top of the cylinder as contrast to the wing-body juncture where the reflection phenomenon causes an increased body lift for a small distance inboard of the juncture.

Whether or not the combination loading will be greater or less than the reference loading for the second definition depends on whether the adverse effect on interference for the body is more than offset by the favorable effect for the wing. Geometrically it depends on two parameters, the wing chord-body radius ratio, and the wing aspect ratio. For the example considered herein the lift of the combination was slightly greater than that of the reference loading based on the blanketed wing area at zero angle of attack.

5.6 Application of $W_{2n}(z)$ Function to Protuberance Pressures for Quasi-Cylindrical Bodies

The $W_{2n}(z)$ functions have useful applications other than wing-body interference. In fact G. N. Ward in Reference (14) uses the $W_o(z)$ function to calculate the pressure on a quasi-cylindrical body of revolution due to surface disturbances which are disturbances of revolution. However with the $W_2(z)$, $W_4(z)$, $W_6(z)$, $W_8(z)$ and $W_{10}(z)$ functions now tabulated, the disturbance may now depend on θ. In fact all that is now necessary is that the disturbances have horizontal and vertical planes of symmetry. The disturbance at any body location can then be expanded in a Fourier Series in $\cos 2n\theta$ on the interval 0 to π as has been done for the interference problem. Equation (40) can then be used to determine the contributions of the Fourier components to the body pressures. If the configuration in question does not possess a horizontal plane of symmetry, the $W_{2n}(z)$ function can still be applied to the part of the configuration for which the upper and lower halves are aerodynamically independent. Not only can the case of protuberances on quasi-cylindrical bodies be treated by the $W_{2n}(z)$ functions, but also the case of supersonic inlets insofar as the inlets meet the symmetry conditions.

5.7 Other Problems Amenable to Treatment by the Methods Presented Herein

The problem of a body at zero angle of attack with a rectangular wing at incidence has been solved. From the pressure distribu-

tions for this case a number of results can be derived. First, the lift and moment results can be determined as a function of both the wing aspect ratio and the ratio of wing chord to body diameter, the two parameters that completely characterize the wing-body combination. The pressure distributions can also be used to determine the minimum drag coefficient of a combination the wing of which has a polygonal cross-section. The pressure distributions can be interpreted as those due to the deflection of a rectangular control surface with a sealed gap.

One of the important problems which is the natural complement of that solved herein, is the determination of the pressures acting on the combination due to unit deflection of the body. (Those due to unit deflection of the wing have been given here). This problem is different from the one already solved in that the interference will not be confined to that part of wing behind the Mach line originating at the leading edge of the juncture. Instead the body will induce upflow across the wing approximately in accordance with Equation (3), and depending on the length of the body in front of the wing, all or part of the wing may be affected. As shown in Figure (3), the problem can be decomposed into several problems (of which the problem solved here is one) including one with the body at zero angle of attack and with the wing twisted. The potential due to the twisted wing can be determined by the usual formula

of supersonic wing theory, Equation (135). If the twisted wing is taken as the wing alone, then a set of Fourier amplitude functions similar to those used here can be determined. With these new amplitude functions, the interference pressure field can be calculated just as in the example considered here. If the new amplitude functions cannot be obtained in closed form, they can always be obtained numerically by harmonic analysis. Once the pressure distribution due to unit angle attack of the body is calculated, the lifting pressures can be readily obtained for a combination with the body and wing at different angles of incidence.

The methods developed here can also be used to determine the pressures due to interference between a circular body and a wing with supersonic edges. For the case of a straight leading edge the Fourier amplitude functions are given in the appendix.

Several extremely important classes of interference problems require the solution of the wing-body problem as a necessary preliminary to their own solution. Specifically these are the problems of wing-tail interference and afterbody pressure distributions. In Reference (22) Lagerstrom and Graham have developed methods for estimating the flow behind the wing of a wing-body combination. These start from a knowledge of the span loading at the wing trailing edge. Since wing-body interference can have an important effect on this span loading, the wing-body problem must be treated first.

VI. CONCLUDING REMARKS

The results that have been presented and discussed in the previous section will not be recapitulated, but rather a few general remarks together with a few suggestions for future work will be given.

In this paper considerable work has been done to get as exact a solution to a wing-body problem as possible. While the numerical results themselves are of considerable interest, it is felt that the value of the work goes further. For one thing much insight has been gained into the actual mechanism of interference. Also exact methods for solving other problems have been developed. Furthermore the exact results will provide a basis for checking the assumptions underlying approximate methods and, when compared with experimental results, will provide a basis for assessing the effects of viscosity on the pressure distributions. The viscous effects will be large for large angles of attack.

Although considerable work is involved in obtaining the complete pressure distributions on a wing-body combination, it should be borne in mind that asking for the pressure distribution is a large order in itself. Considering the complexity of the problem, it is fortunate that any solution at all can be found. From the practical point of view, however, the computations can be performed almost entirely by computers. Considering also the

vast number of engineering hours that go into the design of a complete missile or airplane configuration, some work in determining the pressures acting on the configuration is warranted. However for many purposes an exact solution to the wing-body problem is not necessary. In fact there is at present a very urgent need for a simple approximate method for estimating the pressures acting on wing-body combinations in the region where slender-body theory is known to be inapplicable--a method that will give results of engineering accuracy. It is only hoped that the work here will give some clue how such an urgently needed approximate method can be developed.

REFERENCES

1. C. Ferrari: Interference Between Wing and Body at Supersonic Speeds--Theory and Numerical Application, Jour. of Aero. Sci. (1948), Vol. 15, No. 6, pp. 317-336.

2. C. Ferrari: Interference Between Wing and Body at Supersonic Speeds--Note on Wind-Tunnel Results and Addendum to Calculations. Jour. of Aero. Sci. (1949), Vol. 16, No. 9, pp. 542-546.

3. S. Browne, L. Friedman, and I. Hodes: A Wing-Body Problem in Supersonic Conical Flow (1947), North American Rept. AL-387.

4. P. A. Lagerstrom: Linearized Supersonic Theory of Conical Wings (1948), NACA TN 1685.

5. J. Spreiter: Aerodynamic Properties of Slender Wing-Body Combinations at Subsonic, Transonic, and Supersonic Speeds (1948), NACA TN 1662.

6. J. Spreiter: Aerodynamic Properties of Cruciform-Wing and Body Combinations at Subsonic, Transonic, and Supersonic Speeds (1949), NACA TN 1897.

7. G. Morikawa: The Wing-Body Problem for Linearized Supersonic Flow, Doctoral Dissertation (1949), Calif. Inst. of Tech., Pasadena, Calif.

8. J. Nielsen and F. Matteson: Calculative Method for Estimating the Interference Pressure Field at Zero Lift on a Symmetrical Swept-Back Wing Mounted on a Circular Body (1949), NACA RM A9E19.

9. P. A. Lagerstrom and M. Van Dyke: General Considerations About Planar and Non-Planar Lifting Systems (1949), Douglas Aircraft Co. Rept. No. SM-13432.

10. T. von Karman and N. Moore: The Resistance of Slender Bodies Moving with Supersonic Velocities with Special Reference to Projectiles (1932), Trans. A.S.M.E., Vol. 54, pp. 303-310.

11. H. Tsien: Supersonic Flow Over an Inclined Body of Revolution (1938), Jour. of Aero. Sci., Vol. 5, No. 2, pp. 480-483.

12. J. Cossar and A. Erdelyi: Dictionary of Laplace Transforms (1944-46), Admiralty Computing Service, Dept. of Sci. Res. and Exp., The Admiralty of London, Ref. No. SRE/ACS 53, 68, 71, 102, 108, and Corrections.

13. W. Magnus and F. Oberhettinger: Special Functions of Mathematical Physics (1949), Chelsea Publishing Company, New York, N. Y.

14. G. Ward: The Approximate External and Internal Flow Past a Quasi-Cylindrical Tube Moving at Supersonic Speeds (1948), Q.J. of Mech. and Appl. Math., Vol. I, pp. 225-245.

15. R. Churchhill: Modern Operational Mathematics in Engineering (1944), McGraw-Hill Book Company, Inc., New York, N. Y.

16. G. N. Watson: A Treatise on the Theory of Bessel Functions (1948), Second Edition, The MacMillan Company, New York, N. Y.

17. H. Carslaw and J. Jaeger: Operational Methods in Applied Mathematics (1947), Second Edition, Oxford University Press, London.

18. Admiralty Computing Service: Solution of Some Integral Equations Occurring in an Aerodynamical Problem.

19. Federal Works Agency, W.P.A.: Tables of Sine, Cosine and Exponential Integrals (1940), Vol. I and II.

20. J. Ackeret: Air Forces on Airfoils Moving Faster Than Sound (1925), NACA TM No. 317.

21. E. Jahnke and F. Emde: Tables of Functions (1943) Enlarged and Revised Edition, Dover Publications, New York, N. Y.

22. P. A. Lagerstrom and M. E. Graham: Aerodynamic Interference in Supersonic Missiles (1950), Douglas Aircraft Co. Rept. No. SM-13743.

APPENDIX

Fourier Velocity Amplitudes for Swept Wings

The amplitudes for the Fourier components of the normal velocity at the body for a flat swept wing are given here. Reference should be made to Figure (21) for the coordinate system and wing geometry. The origin of the coordinate system is taken in front of the leading edge of the wing-body juncture for convenience only. The normal velocity at the body surface, q^* , can be expanded in a Fourier series of even multiples of θ with amplitudes depending on z.

$$q^*(z) = \frac{V_0 \alpha_w}{\pi} \sum_{n=0}^{\infty} \tau_{2n}(z) \cos 2n\theta$$

Decomposing $\tau_{2n}(z)$ into parts due to the downwash and sidewash gives the following equation for $\tau_{2n}(z)$

$$\tau_{2n}(z) = a_{2n}(z) + b_{2n}(z)$$

where $a_{2n}(z)$ is the sidewash contribution and $b_{2n}(z)$ is the downwash contribution. The following results have been obtained:

$$a_0(z) = \frac{2}{m\sqrt{m^2-1}}\left[z\sqrt{m^2-1} - \sqrt{1-z^2}\right]; \quad \frac{1}{m} \le z \le 1$$

$$a_0(z) = \frac{2}{m}\left(z - \sqrt{z^2-1}\right) \qquad ; \quad z \ge 1$$

$$b_0(z) = \frac{2}{m}\left(m - \sqrt{(m^2-1)(1-z^2)} - z\right); \quad \frac{1}{m} \le z \le 1$$

$$b_0(z) = \frac{2}{m}\left(m + \sqrt{z^2-1} - z\right) \qquad ; \quad z \ge 1$$

$$a_{2n}(z) = \frac{2}{\sqrt{m^2-1}}\left[\frac{\sin(2n+1)\alpha}{(2n+1)} + \frac{\sin(2n-1)\alpha}{(2n-1)}\right]; \quad \frac{1}{m} \le z \le 1$$

$$\alpha = \cos^{-1}\left(\frac{z}{m} + \frac{\sqrt{(1-z^2)(m^2-1)}}{m}\right)$$

$$b_{2n}(z) = \frac{2\cos(2n-1)\alpha}{(2n-1)} - \frac{2\cos(2n+1)\alpha}{(2n+1)} - \frac{4}{4n^2-1}; \quad \frac{1}{m} \le z \le 1$$

$$a_{2n}(z) = \frac{2(-1)^n}{\sqrt{m^2-1}}\left\{\frac{\left(z-\sqrt{z^2-1}\right)^{2n+1}}{(2n+1)}\cos(2n+1)\sin^{-1}\left(\frac{1}{m}\right)\right.$$

$$\left. - \frac{\left(z-\sqrt{z^2-1}\right)^{2n-1}}{(2n-1)}\cos(2n-1)\sin^{-1}\left(\frac{1}{m}\right)\right\}; \quad z \ge 1$$

$$b_{2n}(z) = 2(-1)^n\left[\frac{\left(z-\sqrt{z^2-1}\right)^{2n-1}}{(2n-1)}\sin(2n-1)\sin^{-1}\left(\frac{1}{m}\right)\right.$$

$$\left. + \frac{\left(z-\sqrt{z^2-1}\right)^{2n+1}}{(2n+1)}\sin(2n+1)\sin^{-1}\left(\frac{1}{m}\right)\right] - \frac{4}{4n^2-1};$$

$$z \ge 1$$

TABLE I

Values of $M_{2n}(z)$

z	$M_o(z)$	$M_2(z)$	$M_4(z)$	$M_6(z)$
0	$-\infty$	$-\infty$	$-\infty$	$-\infty$
.05			-.531	.716
.1	-1.321	-.787	.405	1.334
.15				1.155
.10	-.868	-.166	.902	.735
.25				.279
.30		.131	.831	-.119
.35				-.417
.40	-.538	.304	.560	-.595
.45				-.675
.50			.245	-.655
.6	-.378	.450	-.040	-.417
.7			-.253	-.070
.75				.095
.8	-.292	.457	-.386	.235
.85				.340
.9			-.434	.406
.95				.433
1.0	-.224	.392	-.412	.420
1.1			-.337	.306

z	$M_o(z)$	$M_2(z)$	$M_4(z)$	$M_6(z)$
1.2	-.180	.294	-.231	.123
1.3			-.115	-.062
1.4	-.147	.188	.000	-.197
1.5			.095	-.256
1.6	-.122	.088	.163	-.239
1.7			.204	-.162
1.8	-.102	.005	.211	-.062
1.9			.197	.036
2.0	-.086	-.058	.164	.105
2.1				.134
2.2	-.073	-.100	.069	.121
2.3			.020	.085
2.4	-.062	-.123	-.022	.036
2.5			-.053	-.013
2.6	-.053	-.126	-.073	-.053
2.7				-.063
2.8	-.045	-.119	-.080	-.059
2.9			-.071	-.042
3.0	-.038	-.103	-.060	-.019
3.1			-.038	.005
3.2	-.031	-.083	-.019	.022
3.3			-.002	.030

z	$M_o(z)$	$M_2(z)$	$M_4(z)$	$M_6(z)$
3.4	-.026	-.061	.011	.028
3.5			.021	.019
3.6	-.022	-.040	.027	.008
3.7			.027	-.002
3.8	-.018	-.022	.025	-.011
3.9			.022	-.014
4.0	-.016	-.007	.015	-.013

TABLE II

Values of $W_{2n}(z)$

z	$W_o(z)$	$W_2(z)$	$W_4(z)$	$W_6(z)$	$W_8(z)$	$W_{10}(z)$
0	.500	.500	.500	.500	.500	.500
.05						2.787
.10				2.022	3.136	4.459
.15					3.884	5.264
.20	.4319	.7541	1.644	2.888	4.176	5.164
.25				3.037	4.021	4.213
.30				3.008	3.486	2.857
.35						1.209
.40	.3755	.878	1.929	2.462	1.702	-.345
.50				1.545	-.215	-2.296
.60	.3284	.892	1.428	.508	-1.458	-1.986
.70					-1.697	-.461
.80	.2887	.826	.706	-.940	-1.116	.980
.85						1.317
.90					-.163	1.345
.95						1.107
1.0	.2550	.7056	-.024	-.974	.634	.676
1.1					.930	-.279
1.2	.2262	.557	-.464	-.150	.741	-.803

z	$W_0(z)$	$W_2(z)$	$W_4(z)$	$W_6(z)$	$W_8(z)$	$W_{10}(z)$
1.3						-.638
1.4	.2014	.402	-.558	+.457	-.213	-.045
1.5					-.479	.399
1.6	.1801	.255	-.418	.455	-.514	.475
1.7						.251
1.8	.1616	.128	-.142	.073	.022	-.129
1.9						-.297
2.0	.1454	.026	.081	-.222	.276	-.214
2.1						-.005
2.2	.1313	-.048	.195	-.217	.043	.154
2.3						.167
2.4	.1189	-.097	.196	-.035	-.173	.061
2.5						-.058
2.6	.1080	-.122	.120	.106	-.053	-.108
2.8	.0983	-.128	.025	.098	.075	.007
3.0	.0898	-.122	-.049	-.001		.058
3.2	.0822	-.104	-.078	-.043	-.049	-.066
3.4	.0754	-.082	-.068	-.050	-.030	-.017
3.6	.0693	-.058	-.035	-.008	.011	.022
3.8	.0638	-.035	-.003	.046		
4.0	.0590	-.017		.024		

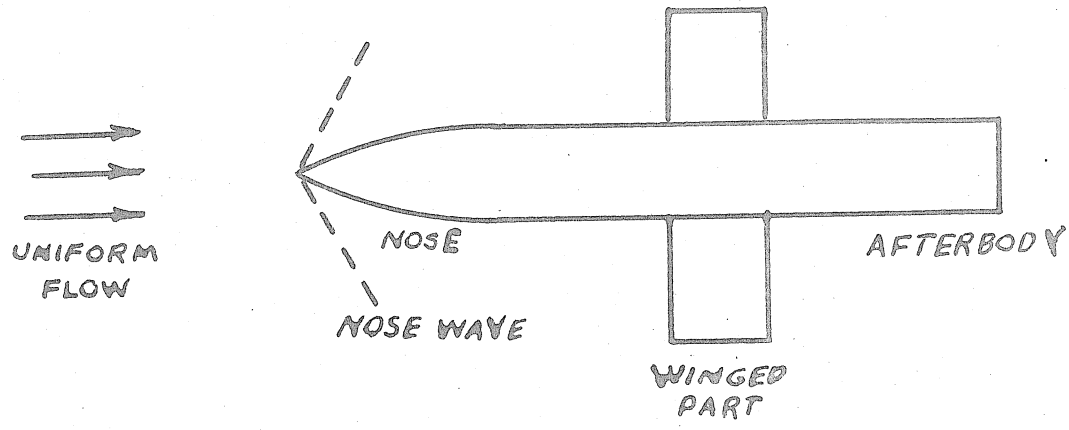

Figure 1. Typical Wing-Body Combination

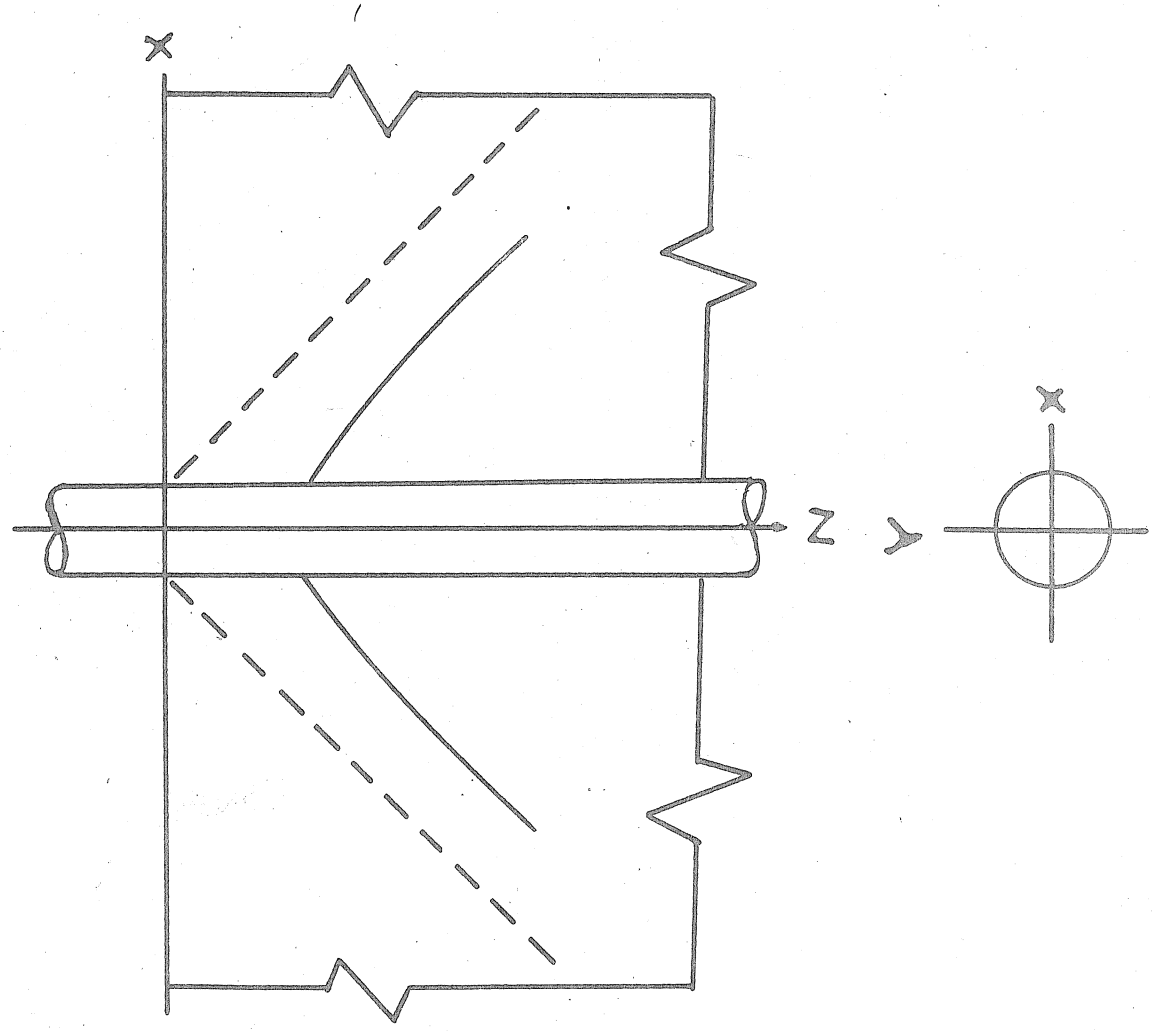

Figure 2. Coordinate System for Wing-Body Combination

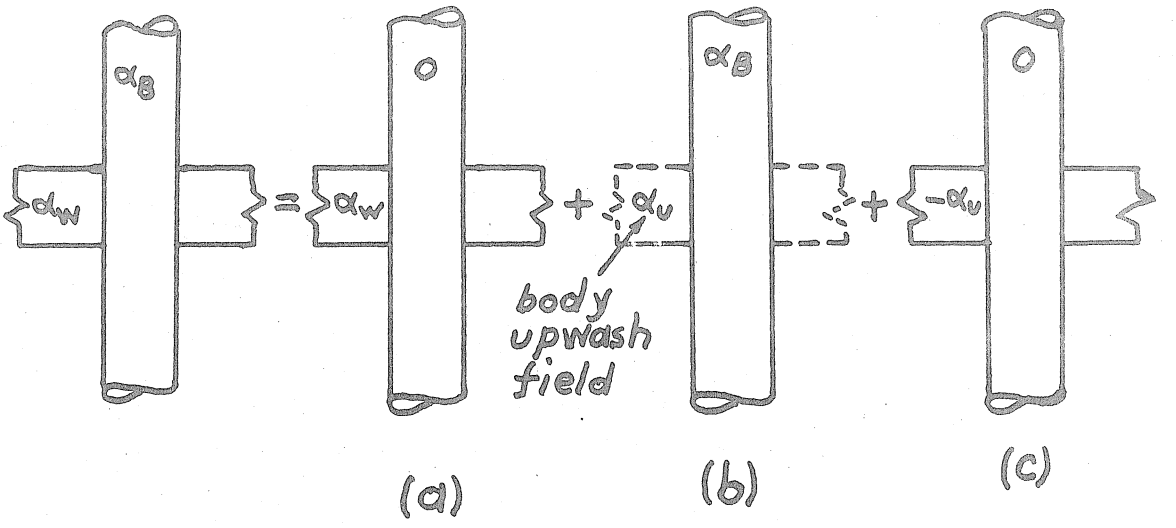

Figure 3. Decomposition of Wing-Body Problem

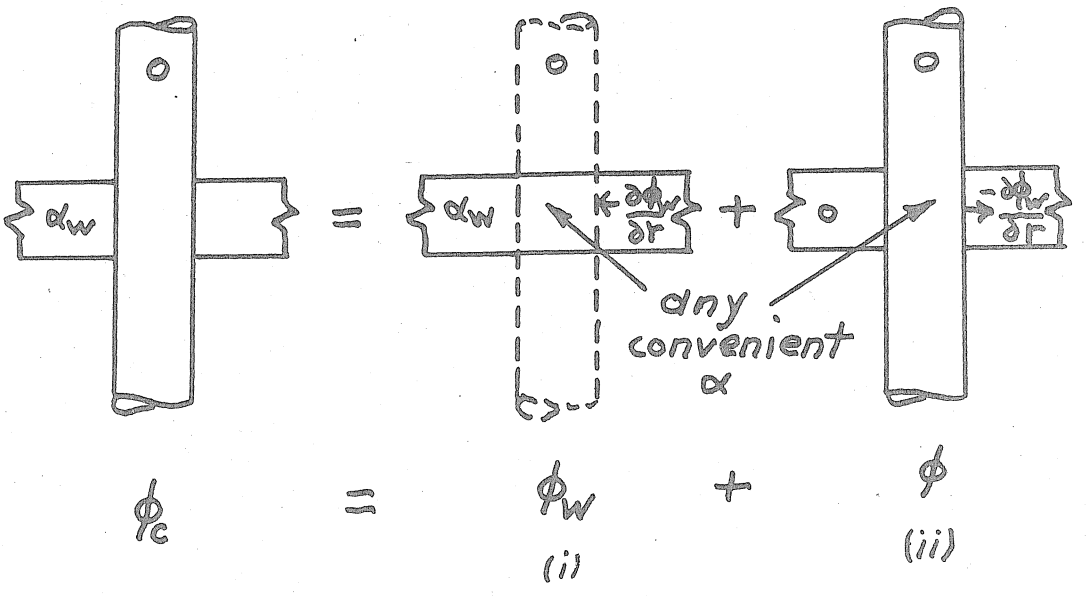

Figure 4. Further Decomposition of a Particular Wing-Body Problem

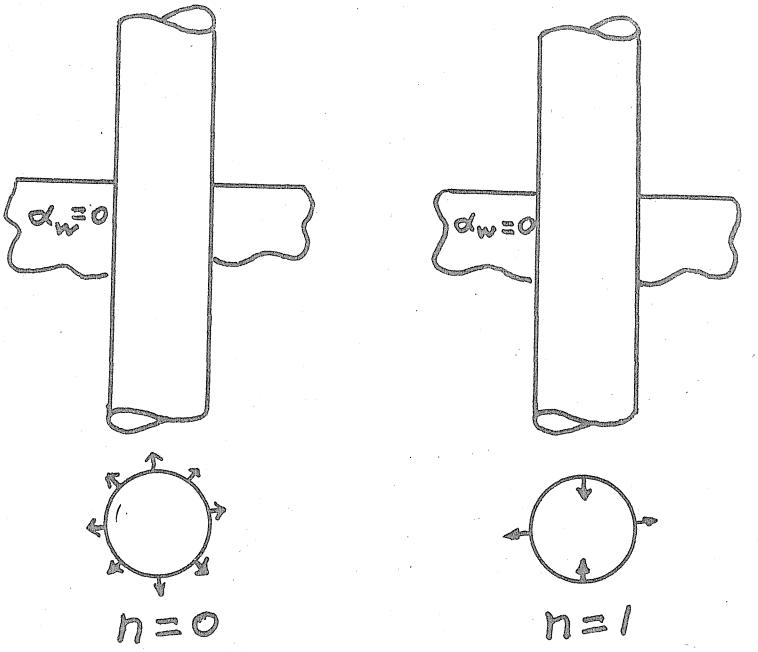

Figure 5. Wing-Body Combinations Corresponding to First Two Fourier Components

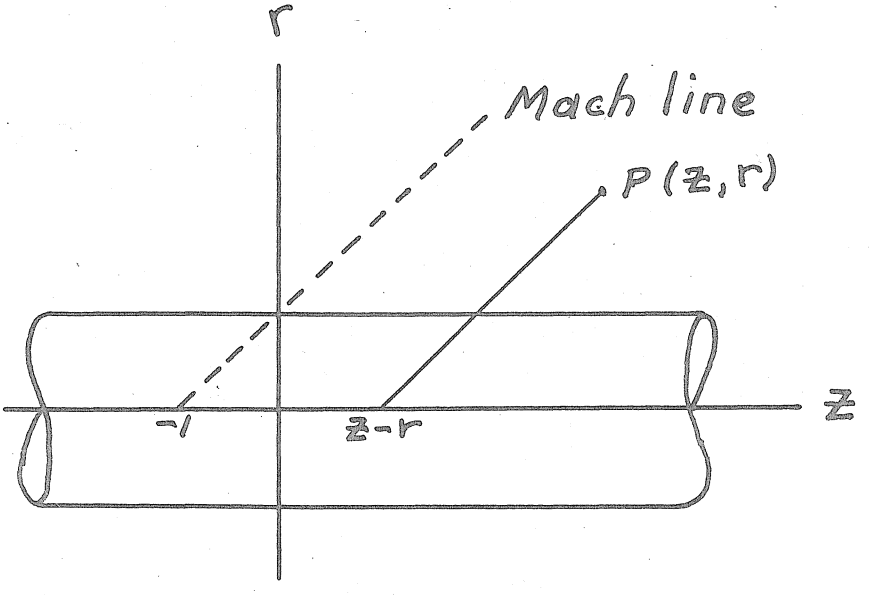

Figure 6. General Point in Interference Field of Wing-Body Combination

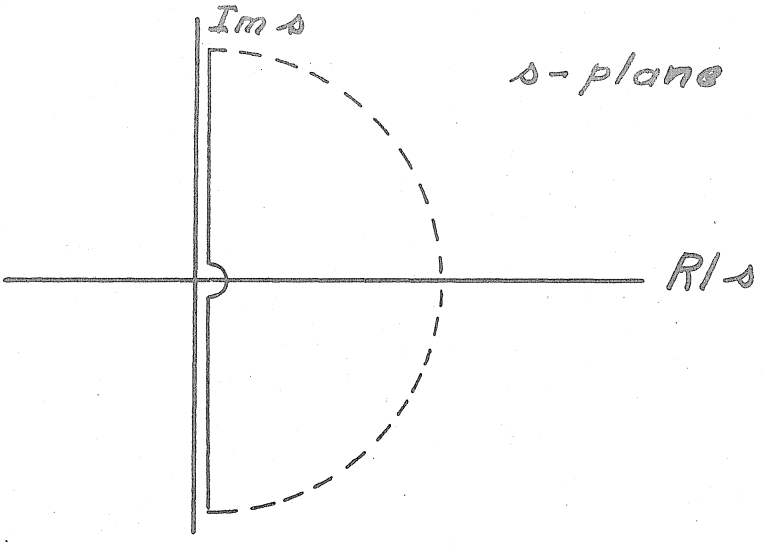

Figure 7. Contour of Integration

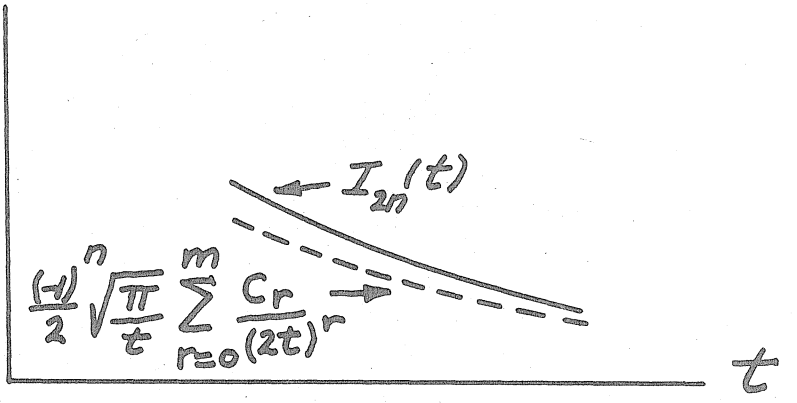

Figure 8. Asymptotic Approximation to Integrand

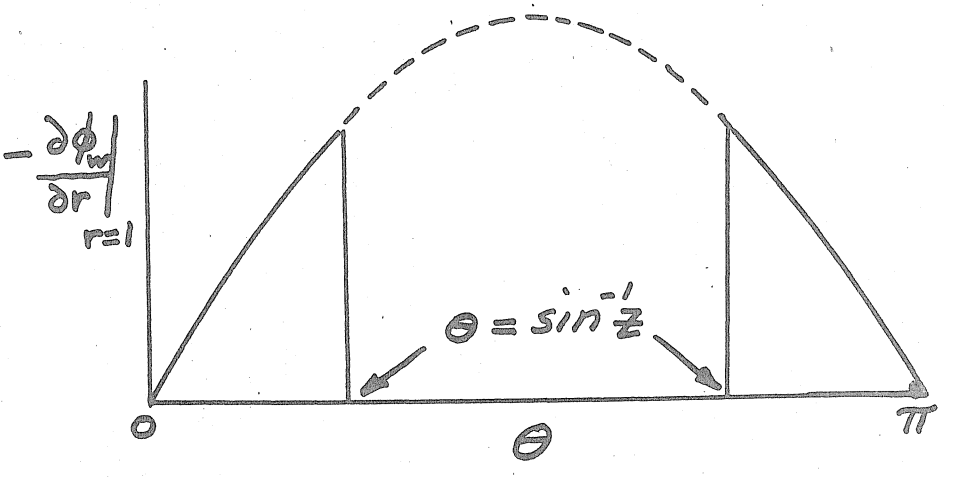

Figure 9. Normal Velocity Distribution at Body Surface

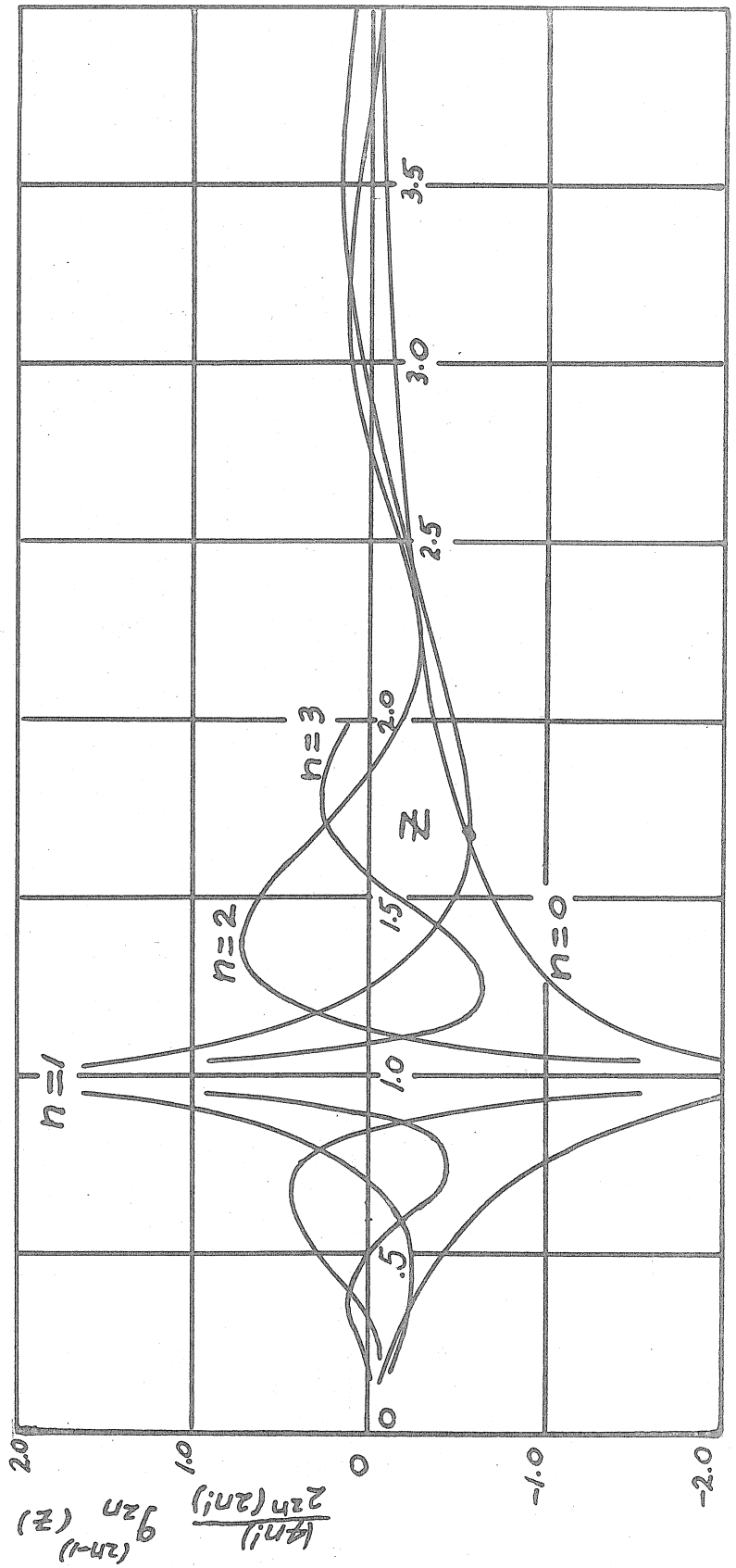

Figure 10. Axial Strength Functions of Fourier Components

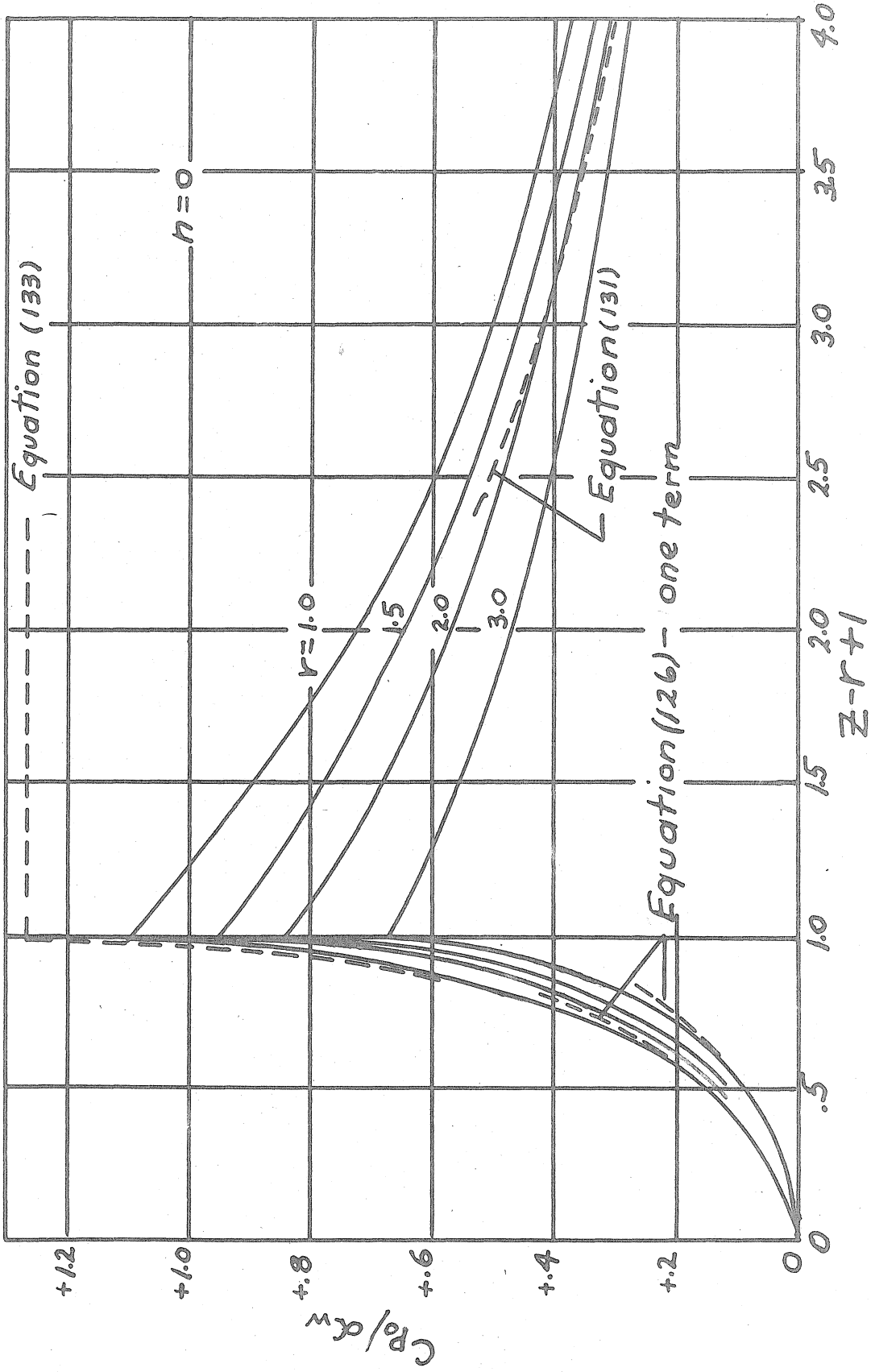

Figure II. Interference Pressure Distributions For First Fourier Component

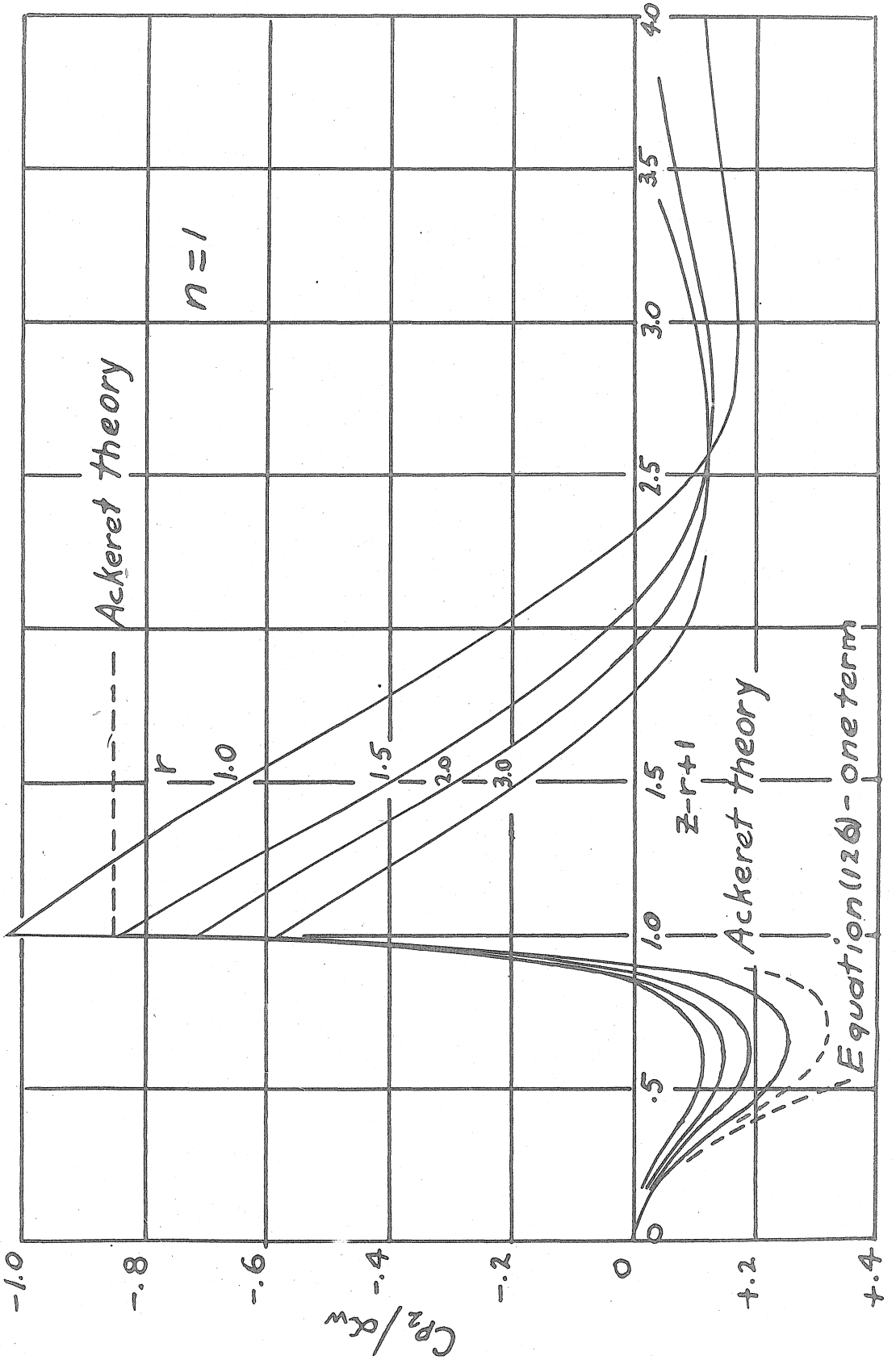

Figure 12. Interference Pressure Distributions For Second Fourier Component

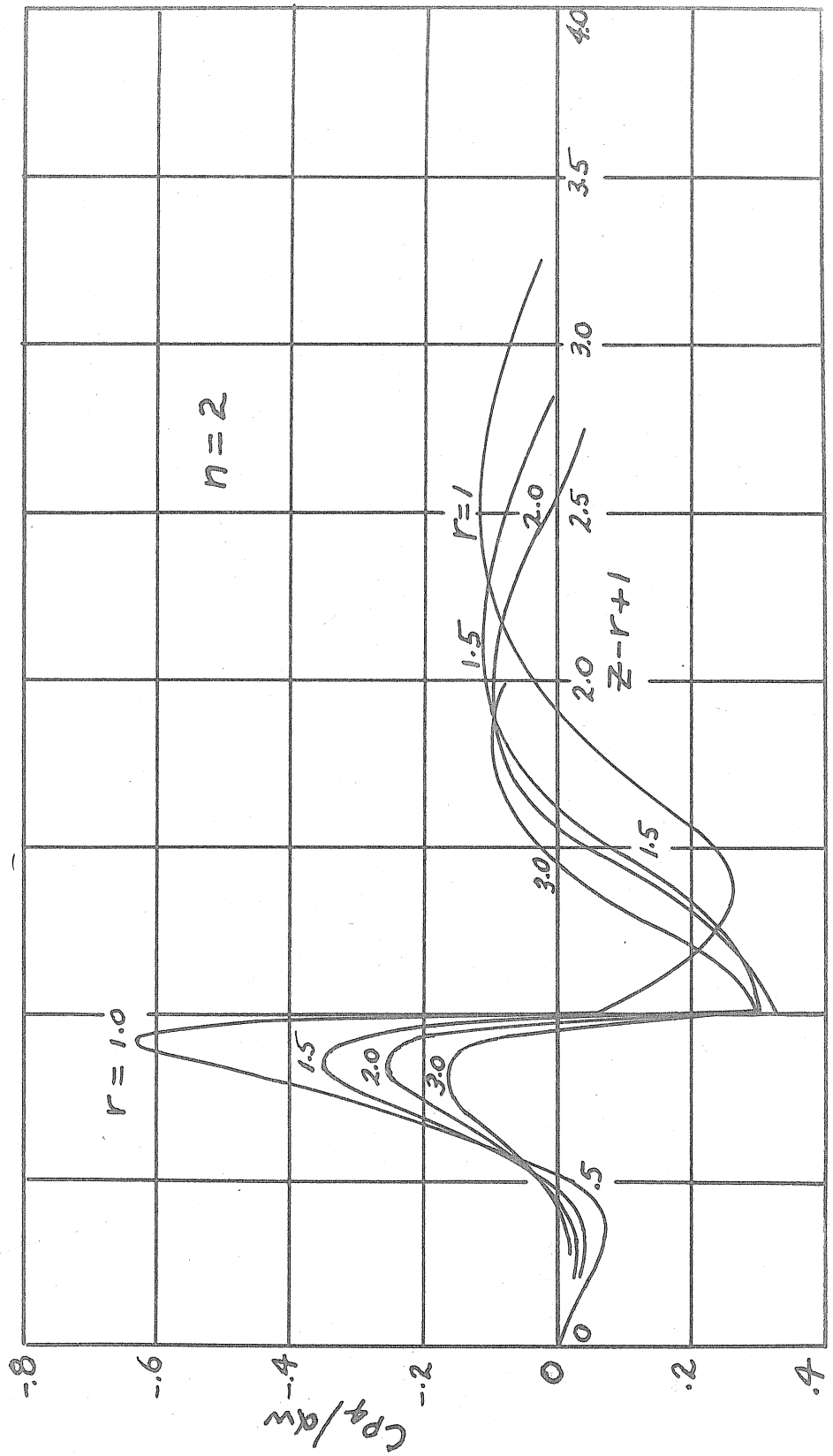

Figure 13. Interference Pressure Distributions For Third Fourier Component

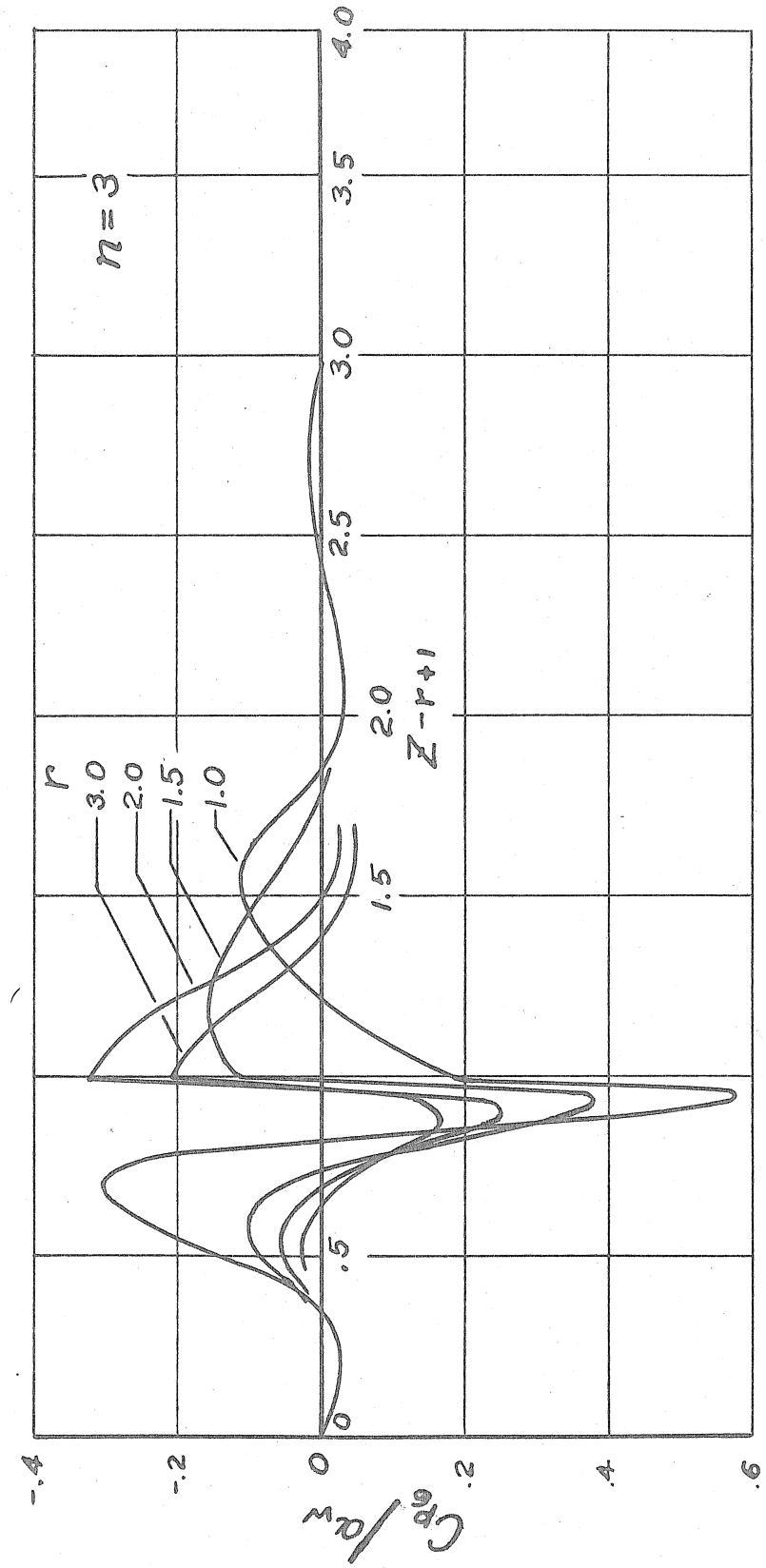

Figure 14. Interference Pressure Distributions For Fourth Fourier Component

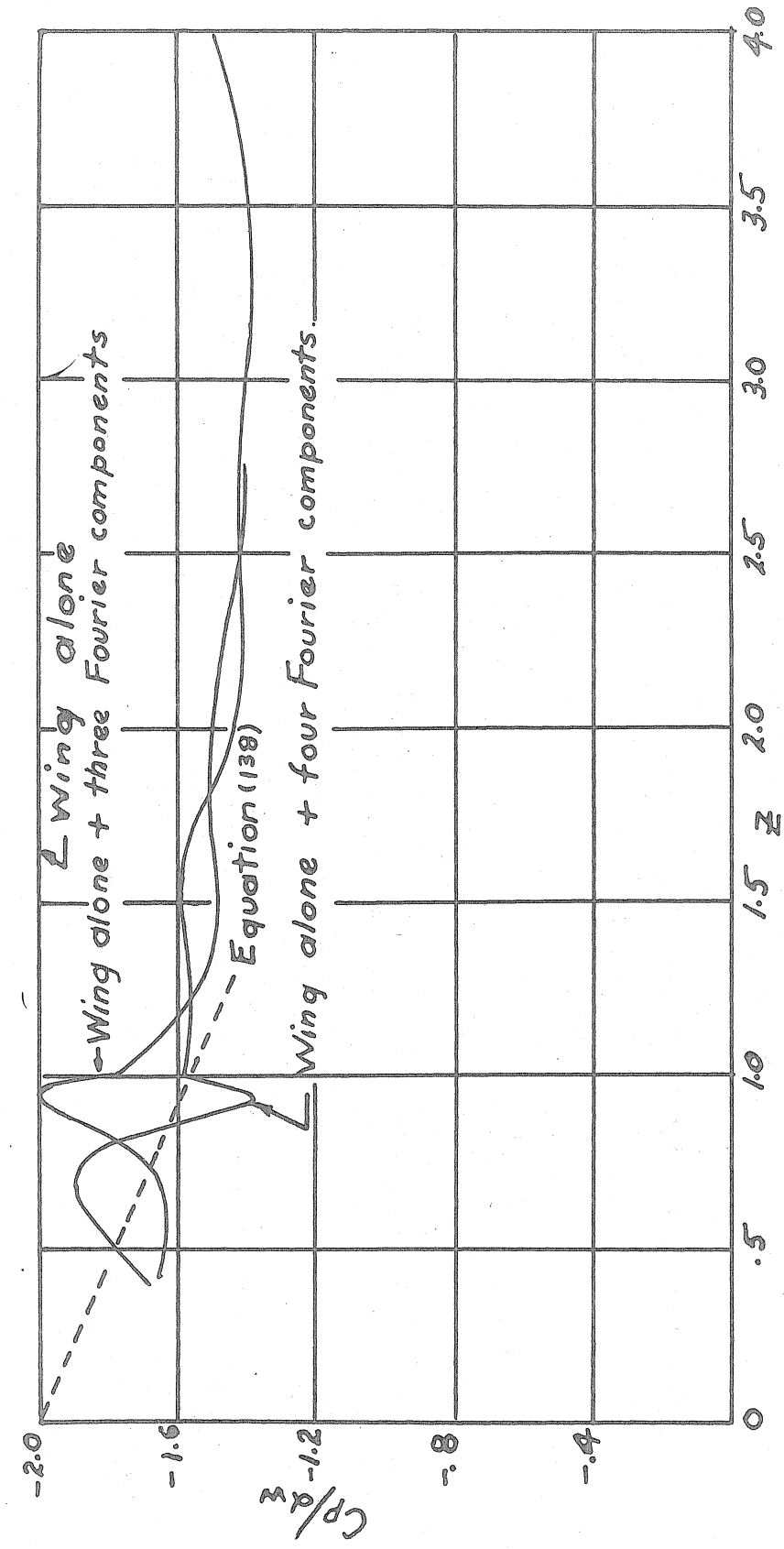

Figure 15. Pressure Distribution at Juncture of Wing-Body Combination

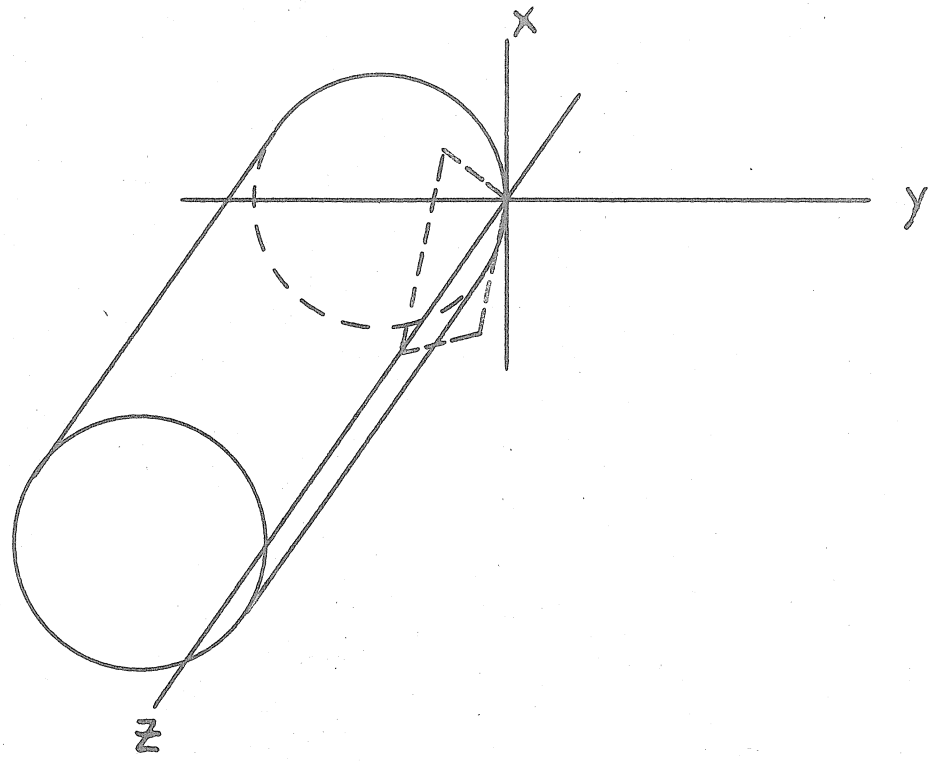

Figure 16. Coordinate System for Equation (135)

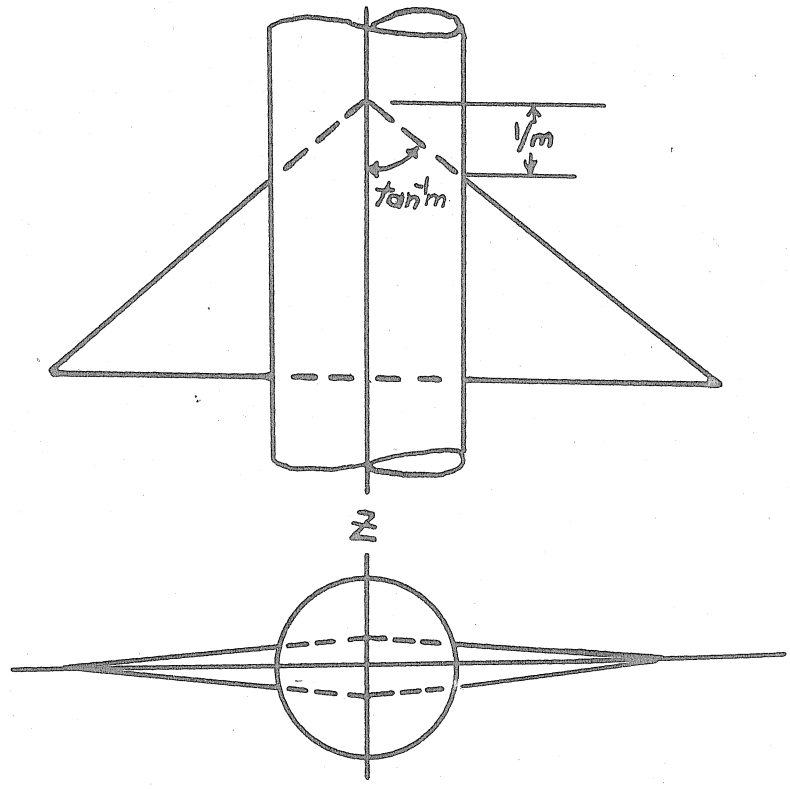

Figure 21. Coordinate System Used in Appendix

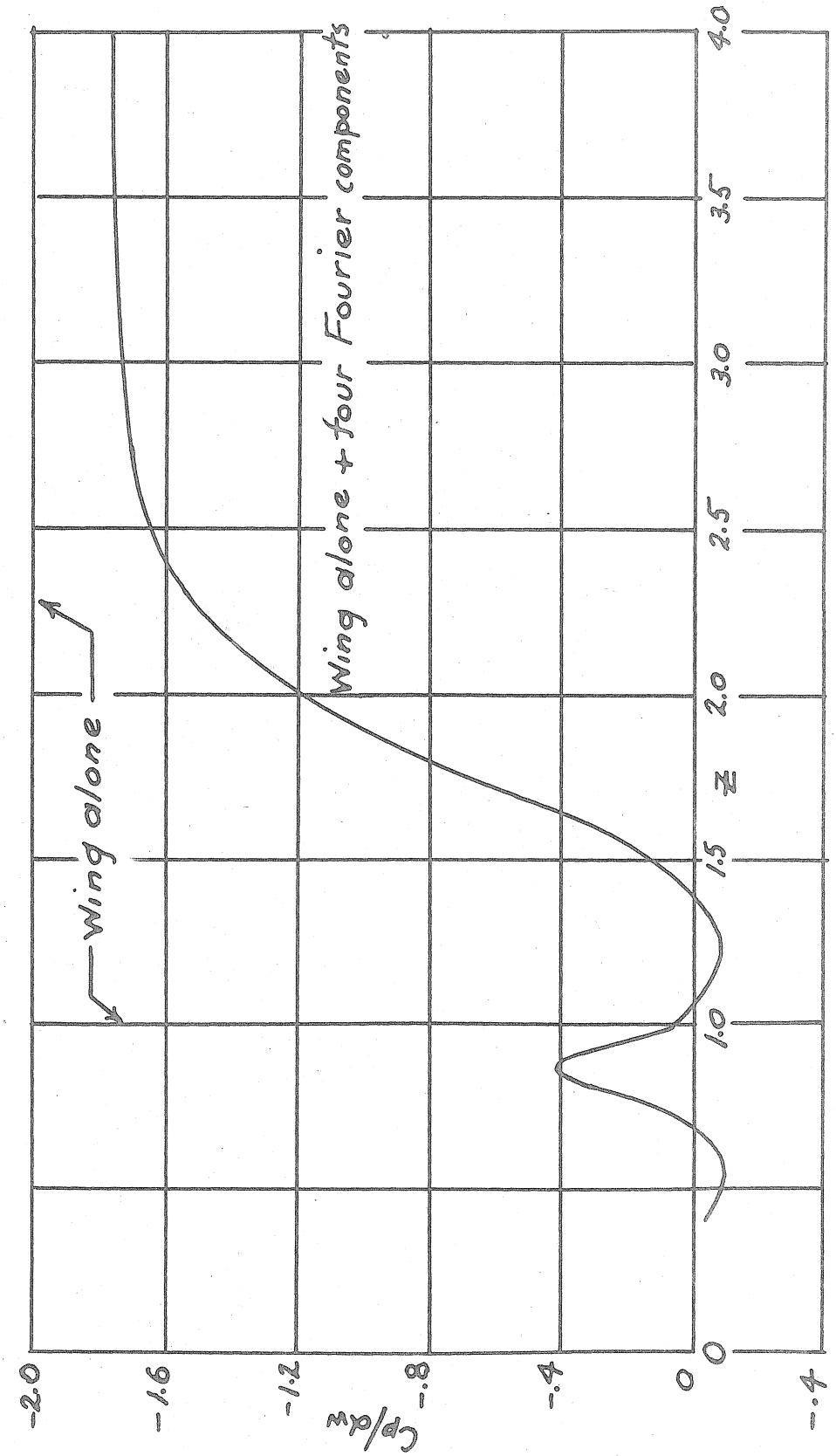

Figure 17. Pressure Distribution at Top of Wing-Body Combination

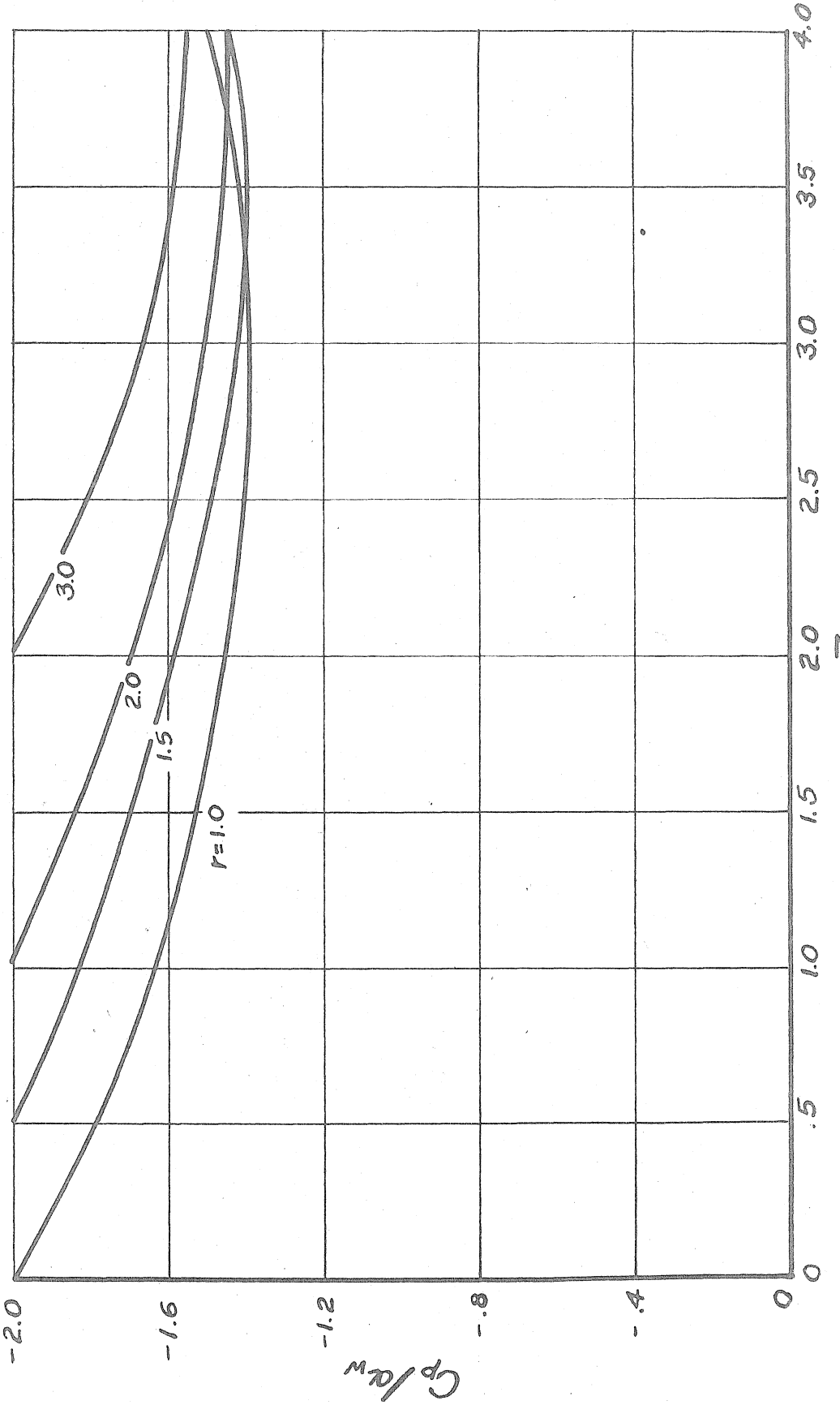

Figure 18. Pressure Distributions for Wing of Wing-Body Combination

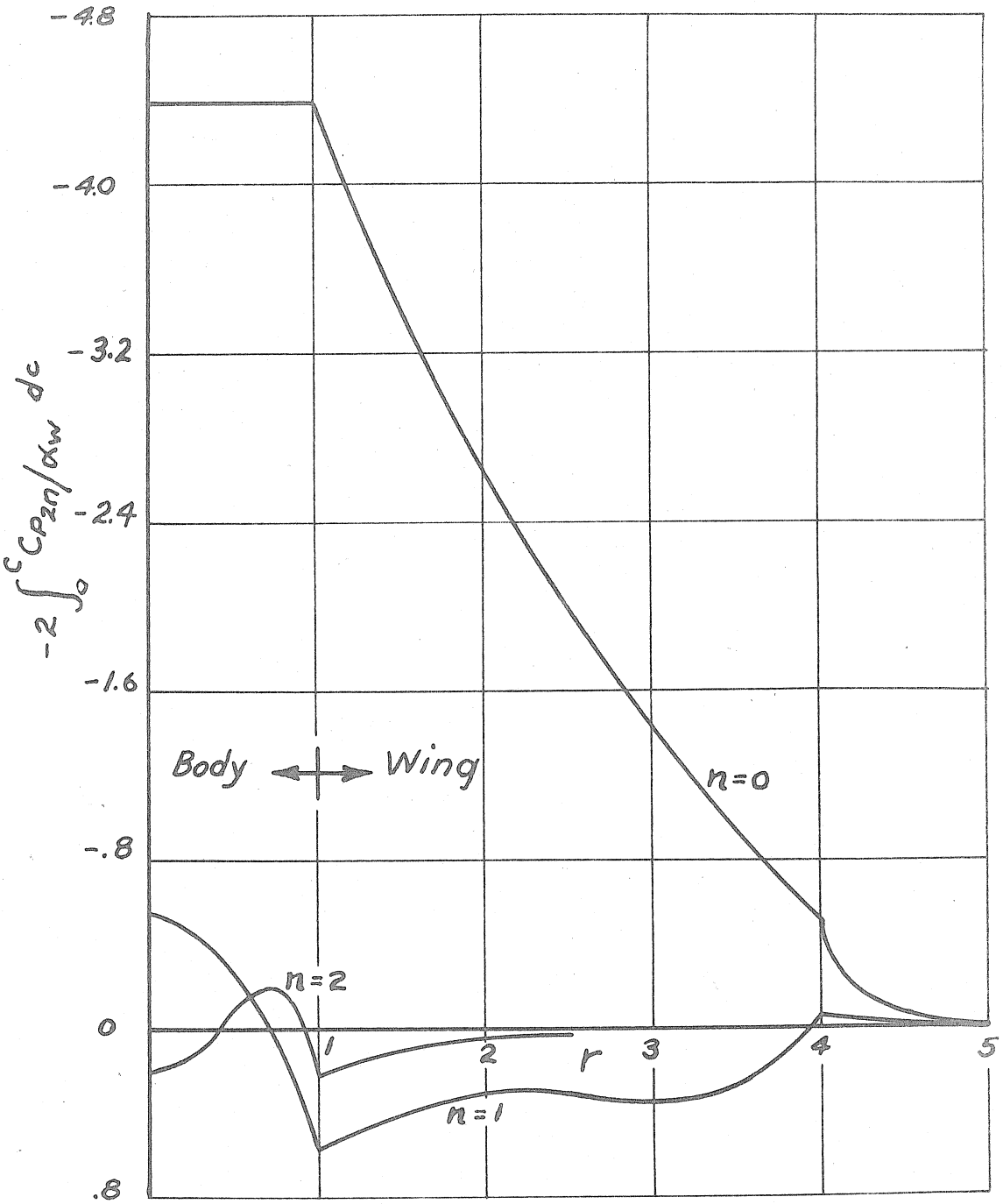

Figure 19. Span Loading of Combination Due to Various Fourier Components

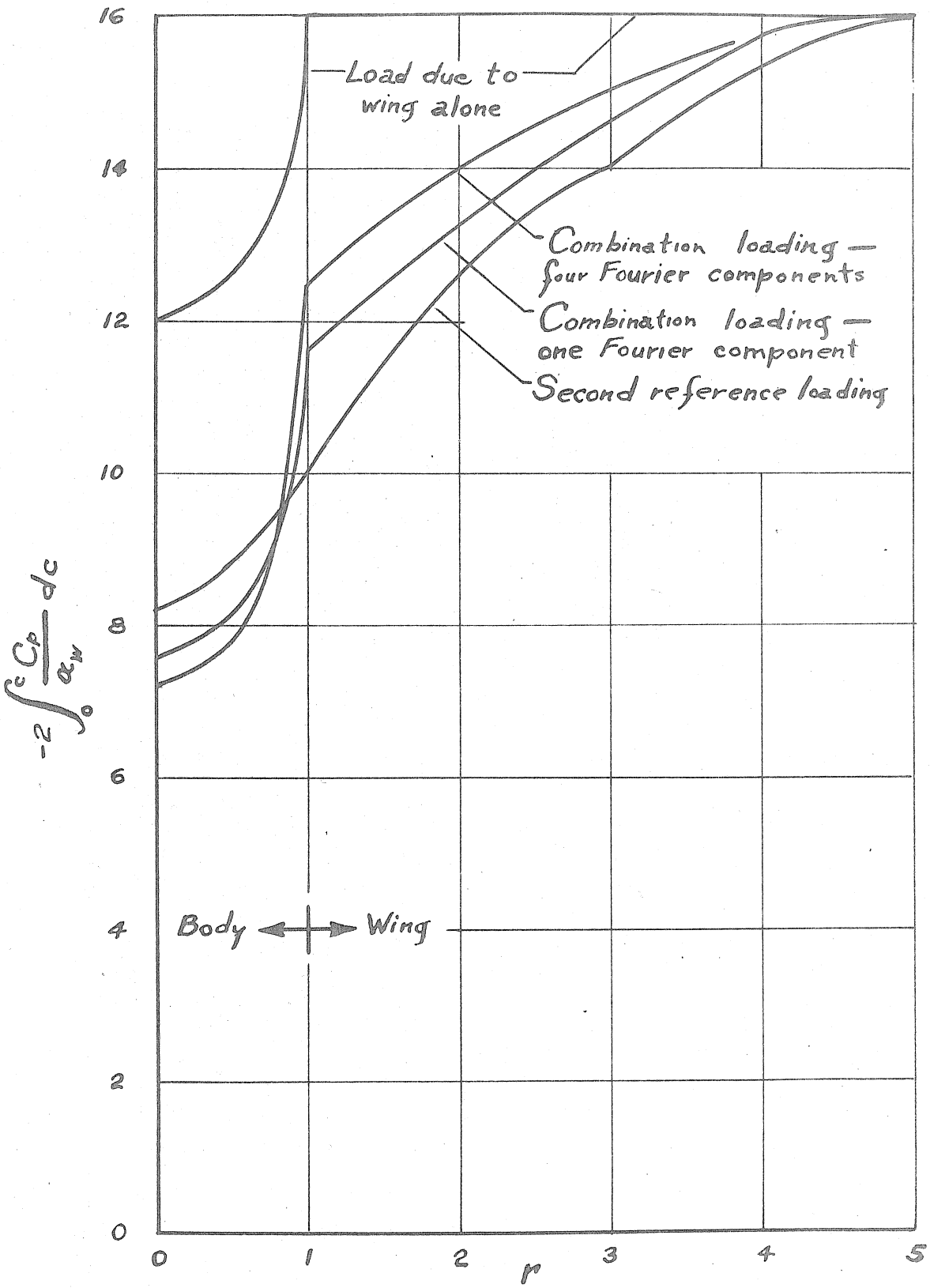

Figure 20. Span Loading of Complete Wing-Body Combination